Carbohydrate Polymers 324 (2024) 121554

Contents lists available at ScienceDirect

Carbohydrate Polymers

journal homepage: www.elsevier.com/locate/carbpol

Structural elucidation of novel pro-inflammatory polysaccharides from *Daphne mezereum* L.

Hussain Shakeel Butt [a,*], Emilie Steinbakk Ulriksen [b], Frode Rise [c], Helle Wangensteen [a], Jens Øllgaard Duus [d], Marit Inngjerdingen [b], Kari Tvete Inngjerdingen [a]

[a] Section for Pharmaceutical Chemistry, Department of Pharmacy, University of Oslo, P.O. Box 1068, Blindern, NO-0316 Oslo, Norway
[b] Department of Pharmacology, Institute of Clinical Medicine, University of Oslo, P.O. Box 1057, Blindern, NO-0316 Oslo, Norway
[c] Department of Chemistry, University of Oslo, P.O. Box 1033, Blindern, NO-0315 Oslo, Norway
[d] Department of Chemistry, Technical University of Denmark, DK-2800 Kgs. Lyngby, Denmark

ARTICLE INFO

Keywords:
Daphne mezereum
Polysaccharides
Pectin
PBMC
TNF-α
IFN-γ

ABSTRACT

Daphne mezereum L., an important medicinal plant in Scandinavian folk medicine, was used to treat ailments such as diarrhea, swelling and stomach pain. A range of natural compounds have been isolated, but little attention has been given to the polysaccharides in this plant. Previous work in our group have shown that a polysaccharide enriched fraction from the bark of *D. mezereum* exhibited pro-inflammatory effects. To pursue this further, the aim of the present work was to isolate and characterize these polysaccharides. From the ethanol-precipitate of a water extract, one neutral (DMP-NF) and one acidic (DMP-AF) fraction was isolated by anion-exchange chromatography. GC, GC–MS and 1D- and 2D-NMR were used to characterize the polysaccharide structures. DMP-NF appeared to be a mixture of arabinan, arabinogalactan and hemicelluloses such as xyloglucan, mannan and xylan. DMP-AF contained a pectic polysaccharide mainly consisting of an unusually long homogalacturonan backbone. Enzymatic treatment by pectinase of DMP-AF yielded DMP-ED, which contained a rhamnogalacturonan-I backbone with arabinan, galactan and arabinogalactan side chains. Both DMP-NF and DMP-ED induced IFN-γ and TNF-α secretion in peripheral blood mononuclear cells (PBMCs), DMP-ED being the most potent fraction. DMP-AF was less active, which might be due to a less sterically available rhamnogalacturonan-I domain.

1. Introduction

In Scandinavian folk medicine, *Daphne mezereum* L. is regarded as an important medicinal plant. Despite its toxicity, infusion of *D. mezereum* was used against several ailments and diseases, such as diarrhea, swelling, stomach pain and tuberculosis (Høeg, 1974; Ulriksen et al., 2022). In addition to Scandinavia, the plant is also native to most of Europe and Western Asia (Moshiashvili, Tabatadze, & Mshvildadze, 2020). Several compounds from *D. mezereum* have been isolated and characterized, such as the coumarin glycosides triumbellin (Kreher, Wagner, & Neszmélyi, 1990), daphnorin (Tschesche, Schacht, & Legler, 1963), and the diterpene esters gniditrin (Görick & Melzig, 2013) and mezerein (Kupchan & Baxter, 1975). However, the polysaccharides from the Daphne genus have been given little attention.

Polysaccharides are a group of biopolymers that has gained an increased interest due to their interesting biological properties. This includes antitumor (Huang, Chen, Yang, & Huang, 2021), immunomodulatory (Gao et al., 2020) and antiviral (T. Wang et al., 2020) activity. For instance, the β-glucan lentinan extracted from the medicinal mushroom *Lentinula edodes* (Shiitake), has shown improved overall response rates against lung cancer in combination with chemotherapy due to its ability to stimulate immune cells (Y. Zhang et al., 2018). Another type of polysaccharide that is studied extensively for immunomodulatory effects is plant-derived pectins.

Pectins are a group of polysaccharides found in the middle lamella or the primary and secondary cell wall in plants. They are characterized by their high content of D-galacturonic acid (GalA). The backbone of pectins is suggested to consist of linear homogalacturonan (HG) and two branched rhamnogalacturonan (RG) regions, namely RG-I and RG-II (Wusigale, Liang, & Luo, 2020). In the HG-region, the partially acetylated or methyl-esterified GalA units are α-(1,4)-linked. In the RG-I region, the backbone is made up of rhamnose (Rha) and GalA residues that

* Corresponding author at: Department of Pharmacy, University of Oslo, P.O.Box 1068, Blindern, 0316 Oslo, Norway.
E-mail address: h.s.butt@farmasi.uio.no (H.S. Butt).

https://doi.org/10.1016/j.carbpol.2023.121554
Received 20 June 2023; Received in revised form 30 October 2023; Accepted 31 October 2023
Available online 3 November 2023

are linked in the following manner: [−4)-α-D-GalA-(1,2)-α-L-Rha-(1]$_n$. Branching occurs at the O4-position of the rhamnose units. These side chains may be arabinans, galactans or arabinogalactans (Maxwell, Belshaw, Waldron, & Morris, 2012). The RG-II region on the other hand consists of minimum eight α-(1,4)-GalA units. It is a highly complexed branched region which consists of unusual sugars such as apiose, 2-*O*-methyl fucose and 3-deoxy-D-manno-2-octulsonic acid (Bonnin, Garnier, & Ralet, 2014).

Immunomodulation by pectins may occur in a direct manner or indirectly through their role as dietary fibers. Pectins are not degraded by either human saliva, gastric acid or by human digestive system, and are therefore transferred undigested to the colon. Here, the gut microbiota degrades the pectin into the short fatty acids acetate, propionate and butyrate, all of which have displayed health promoting benefits (Koropatkin, Cameron, & Martens, 2012). Butyrate, for instance, is thought to exert modulatory effects on gut immune function (Siddiqui & Cresci, 2021). Further, by interacting with toll like receptors (TLRs), a type of pattern recognition receptors (PRRs) on immune cells, pectins can directly affect the immune cell response. A study on pectins with low degree of methyl esterification (DM) suggested that they may inhibit the pro-inflammatory TLR2-TLR1 pathway by binding to TLR2 through electrostatic interactions between non-esterified galacturonic acids on the pectin and positive charges on the TLR2 ectodomain (Sahasrabudhe et al., 2018). However, the TLR2-TLR6 pathway did not appear to be affected by this, which is probably due to hydrophobic interactions being predominant in this pathway.

A recent study indicated that pectins may also activate macrophages by interacting with TLR4 and complement receptor 3. By interacting with TLR4, the pectin activates myeloid differentiation protein 88 through IL-1 receptor kinase, followed by activation of TNF-receptor associated factor, MAPKs and NF-κB. The latter two are also activated by complement receptor 3, but through the activation of phosphoinositide-3-kinase and protein kinase C. The overall effect of the pectic interactions led to enhanced phagocytosis and pinocytosis, in addition to the release of IL-1β, TNF-α, IL-6 and NO (Huang et al., 2021). Other studies have also obtained similar results (H. Wang et al., 2018; Wang et al., 2019). Pectins with both a low and a high DM have been reported to activate TLR4 (Prado et al., 2020).

Earlier studies have shown that a crude polysaccharide extract from *Daphne pseudogenkwa* exhibits interesting antitumor properties (Moon, Park, Lee, & Yoon, 1985). Furthermore, we have preliminary results of a polysaccharide enriched fraction from *D. mezereum* showing promising stimulatory effects of macrophages and peripheral blood mononuclear cells (PBMCs) (Ulriksen et al., 2022). The fraction contained significant amounts of GalA, in addition to the presence of arabinose (Ara) and galactose (Gal), which could indicate the presence of pectic polysaccharides. However, no detailed structural characterization of purified polysaccharides from *D. mezereum* exist. Based on this, the aim of this study was to further isolate and structurally characterize polysaccharides from *D. mezereum*, and explore their immunostimulant effects on human PBMCs.

2. Methods

2.1. Plant material

Bark from *Daphne mezereum* L. (family: Thymelaeaceae) was collected 15.04.21, near Sognsvann in Oslo (59°57′55"N 10°42′30″E), Norway and its identity was verified by associate professor Anneleen Kool (Natural History Museum, UiO, Norway). The bark was airdried and pulverized using a kitchen blender (Vitamix A2300i). A voucher specimen with number RL-202120415-dm was deposited at the Natural History Museum herbarium.

2.2. Extraction of polysaccharides

A water extract of the plant material was obtained using an accelerated solvent extraction (ASE) 350 instrument (Dionex, Sunnyvale, CA, USA) at 100 °C with dH_2O as extraction solvent. Each cell was filled with 10 g of plant material and extracted twice with dH_2O. The water extract was applied to a Diaion HP-20 column (5 × 50 cm) and eluted with three column volumes of dH_2O. The obtained water fraction was further added 3-fold volumes of ethanol and kept at 4 °C for 48 h in order to precipitate the polysaccharides. The precipitate was washed with ethanol, centrifuged (4400 rpm, 20 min) and filtrated using a Büchner funnel. The precipitate was washed with ethanol, centrifuged (4400 rpm, 5 min) and filtrated again. Finally, the precipitate was washed with acetone, dried at room temperature, dissolved in water and freeze dried for 48 h in order to obtain a polysaccharide fraction, which will be furthered referred to as DMP (***D**aphne **M**ezereum* **P**olysaccharide).

2.3. Fractionation of polysaccharides

The extraction and fractionation procedure used for obtaining the isolated polysaccharides is illustrated in Fig. 1. All fractions were filtered through 0.45 μm Millipore filters before they were applied to the columns.

2.3.1. Anion-exchange chromatography

A solution of DMP (5 mg/mL in dH_2O) was applied to a column packed with ANX Sepharose™ 4 Fast Flow (high sub) (GE Healthcare, 5 × 25 cm). The column was eluted with degassed dH_2O (1 mL/min) to obtain a neutral fraction (DMP-NF), followed by a linear NaCl gradient (0–1.5 M, 2 mL/min) to give an acidic fraction (DMP-AF). The collection volume was 10 mL/tube. The carbohydrate elution profile was determined using the phenol-sulfuric acid method (DuBois, Gilles, Hamilton, Rebers, & Smith, 1956). The relevant fractions were pooled and dialyzed against dH_2O (cut-off 3500 Da), and freeze-dried for 48.

2.3.2. Size exclusion chromatography

DMP-NF (5 mg/mL in dH_2O) was applied to a Sephacryl S100 HR column (Pharmacia, 2 × 55 cm), eluted with degassed dH_2O (0.5 mL/min) and volumes of 1 mL/tube were collected. The carbohydrate elution profile was determined using the phenol-sulfuric acid method (DuBois et al., 1956). The relevant fractions were pooled and freeze-dried for 48 h. The size exclusion column chromatography experiment was performed using an Äkta FPLC system (Pharmacia Äkta, Amersham Pharmacia Biotech) with a fraction collector. The Unicorn 4.0 software (GE Healthcare) was used to set up and monitor experiments.

2.4. Enzymatic degradation by pectinase

DMP-AF (200 mg) was dissolved in minimal volume acetate buffer (50 mM, pH = 4) and added pectinase from *Aspergillus niger* (200 μL, 55 U/mg, Sigma Aldrich). One unit of pectinase liberates 1 μmol of GalA from polygalacturonic acid per min at pH 4.0 at 25 °C. The solution was incubated at 25 °C for 24 h. Additional pectinase (20 μL) was added after 8 h. The solution was brought to boil in order to denature the enzyme, cooled down and applied to a HiLoad™ 16/60 Superdex™ 200 prep grade column (GE Healthcare, 16 × 60 cm). The column was eluted with degassed dH_2O at 0.5 mL/min and fractions were collected (2 mL/tube). Based on the phenol-sulfuric acid assay, the relevant fractions were pooled and freeze-dried for 48 h, and an enzymatically degraded product (DMP-ED) was obtained. The size exclusion column chromatography experiment was performed using an Äkta FPLC system (Pharmacia Äkta, Amersham Pharmacia Biotech) with a fraction collector. The Unicorn 4.0 software (GE Healthcare) was used to set up and monitor experiments.

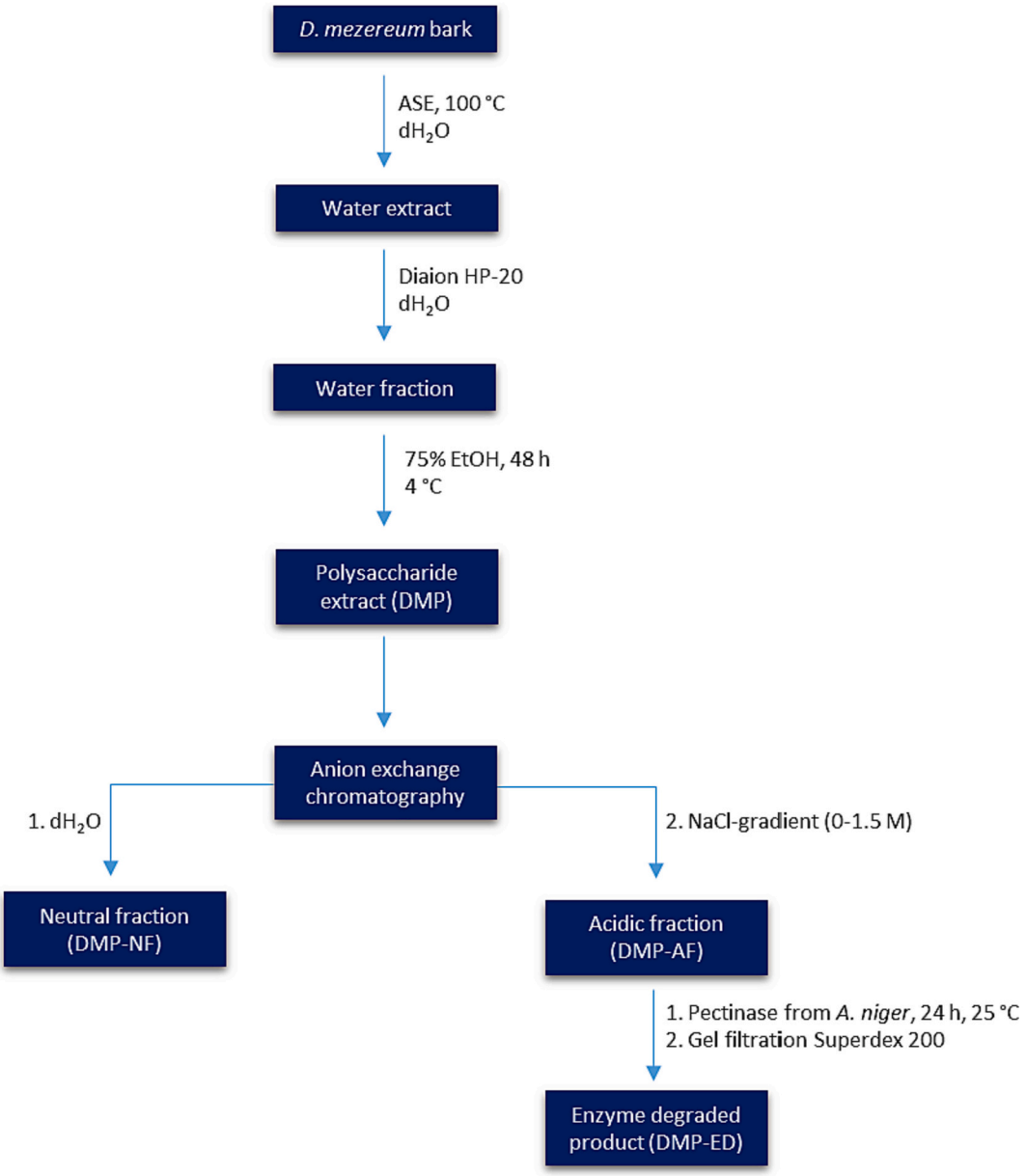

Fig. 1. Flowchart for extraction and fractionation of polysaccharides from the bark of *D. mezereum.*

2.5. Determination of monosaccharide composition

The monosaccharide composition was determined as previously described (Chambers & Clamp, 1971; Ulriksen et al., 2022). In short, the samples were subjected to 3 M HCl in anhydrous methanol for 24 h at 80 °C. Trimethylsilylated derivatives of the methyl glycosides obtained after methanolysis were analyzed using a Restek RTx-5 silica column (30 m, i.d. 0.25 mm, 0.25 μm film thickness) coupled to a Focus GC (ThermoFisher Scientific, Waltham, MA) with a flame-ionization detection. The parameters used for the gas chromatography were identical to previous studies (Wold et al., 2018). Helium was used as a carrier gas and Chromeleon software v.6.80 (Dionex Corporation, Sunnyvale, CA) was used to analyze the results. Mannitol was used as an internal standard.

2.6. Linkage analysis

Glycosidic linkage analysis was performed as described earlier (Pettolino, Walsh, Fincher, & Bacic, 2012; Wold et al., 2018). All samples were subjected to carboxyl reduction prior to methylation. In short, the samples were reduced by $NaBD_4$, and methylated by NaOH in DMSO and methyl iodide. This was followed by hydrolysis by trifluoroacetic acid and a subsequent reduction by $NaBD_4$. Finally, acetylation was achieved by adding 1-methylimidazole and acetic anhydride. The partially methylated samples were analyzed by GCMS-QP2010 (Shimadzu Corporation) with a Restek Rxi-5MS silica column (30 m, i.d. 0.25 mm, 0.25 μm film thickness), split injection and set at a constant pressure mode. Initial flow was 1 mL/min. The injector and interface temperatures were 280 °C. At the time of injection, the column temperature was 80 °C. After 5 min, the temperature was increased with

10 °C/min up to 140 °C. This was later followed by increase of 4 °C/min to 210 °C and lastly 20 °C/min to 310 °C, where it was kept for 4 min. Helium was used as a carrier gas, and the temperature of the ion source was 200 °C. Spectra were analyzed using GC–MS solution software, v.2.10 (Shimadzu Corporation).

2.7. Precipitation with β-Yariv glucosyl reagent

The presence of arabinogalactan type-II was determined for DMP-NF, DMP-AsF and DMP-ED by precipitation with β-Yariv glucosyl reagent by single radial diffusion with arabic gum (1 mg/mL in dH_2O) as a positive control (van Holst & Clarke, 1985). In short, 3.5 mL of a solution containing 0.02% (*w/v*) sodium azide, 0.86% (w/v) sodium chloride and 1% (w/v) agarose in dH_2O was heated to boiling. β-Yariv glucosyl reagent (100 μL, 2 mg/mL) was added before the solution was poured onto a gel bond film (5 × 7 cm) and allowed to cool down. All samples were made in concentrations of 2 mg/mL and 4 mg/mL in dH_2O. Three wells were made for each concentration of each sample using a gel puncher. The wells were filled with either 2, 4 or 6 μL of each solution. The gel bond film was placed in a moist chamber overnight. A colored precipitate is formed with compounds containing AG-II structures.

2.8. Iodine-starch test

The presence of starch was determined for DMP-NF, DMP-AF and DMP-ED by adding a few drops of aqueous iodine-potassium-iodide solution to each fraction (Hunter, McIntyre, & McIlroy, 1970). Starch from potato (Sigma Aldrich) was used as a positive control and dH_2O as a negative control. A positive reaction gives a dark bluish color. The presence of starch was visually determined by comparing all of the solutions.

2.9. Determination of 3-deoxy-D-manno-2-octulosonic acid

The presence of 3-deoxy-D-manno-2-octulosonic acid (KDO) was determined for DMP-AF and DMP-ED with KDO as positive control as described previously (Karkhanis, Zeltner, Jackson, & Carlo, 1978). In short, each sample (100 μL, 0.1 mg/mL in dH_2O) was transferred to a pyrex tube, added dH_2O (150 μL) and H_2SO_4 (250 μL, 0.2 M), before being heated for 30 min at 100 °C. The solutions were cooled down, centrifuged (3000 rpm, 5 min) and 500 μL of the supernatant was transferred to a new pyrex tube followed by addition of HIO_4 (250 μL, 0.04 M in 62.5 mM H_2SO_4). The samples were incubated for 20 min. Each tube were added a fresh solution of Na_2SO_3 (500 μL, 2% in HCl), vortexed and incubated until the brown color disappeared. Then, a solution of thiobarbituric acid (500 μL, pH = 3, 0.6% in dH_2O) was transferred to each tube and heated for 15 min at 100 °C. The samples were taken out and DMSO (1 mL) was immediately added to each solution. Finally, the samples were cooled down and the absorbance was measured at 548 nm using a Molecular Devices FlexStation 3 Reader.

2.10. Molecular weight determination

The average molecular weight (M_W) of each sample was determined as described earlier (Fu et al., 2022). In short, each fraction (2 mg/mL, 0.5 mL) was applied to a Superose™ 6 column (Amersham Biosciences, 1 × 30 cm) and eluted with NaCl (10 mM, 0.5 mL/min). The collection volume was 0.5 mL/tube. The M_W of all samples were calculated using a calibration curve where the logarithmic value of M_W of different dextran polymers (5.6, 80, 150, 233 and 475 kDa) was plotted against the fraction tube number.

2.11. Nuclear magnetic resonance (NMR) spectroscopy

Fractions (5–10 mg) were dissolved in D_2O (500 μL, 99.9%, Sigma) and sodium 2,2-dimethyl-2-silapentane-5-sulfonate (Sigma) was used as the reference compound. All experiments were carried out on a Bruker Advance III HD 800 MHz spectrometer quipped with a 5-mm cryogenic CP-TCI z-gradient probe at 333.15 K (Bruker, Rheinstetten, Germany). The following spectra were recorded using TopSpin 3.5 with or without CW presaturation for suppression of water signals: ^{1}H NMR (continuous-wave presaturation, pulse program "zgpr"), ^{13}C NMR (pulse program "zrestse.dp.jcm800"), phase sensitive COSY (pulse program "cosygpprqf"), TOCSY (pulse program "dipsi2hpr", 80 ms mixing time), ROESY (pulse program "roesyph", mixing time 250 ms), NOESY (pulse program "awnoesygppr", 250 ms mixing time), HSQC (pulse program "awhsqcedetgpsisp2.3–135pr" and "awhsqc135pr") and HMBC (pulse program "awhmbcgplpndqfpr" and "awshmbcctetgp12nd.m"). Spectra were processed and analyzed using TopSpin 3.6.2 software (Bruker).

2.12. Determination of the degree of methylation and acetylation

The degree of methylation (DM) and acetylation (DAc) of the pectin in DMP-AF was determined by a quantitative ^{1}H NMR method described by Müller-Maatsch, Caligiani, Tedeschi, Elst, & Sforza, 2014. In short 10 mg of DMP-AF was incubated at 2 h in room temperature with 1 mL 0.4 M NaOH in D_2O. 4 μL of a 5%-solution of TSP in D_2O was added as internal standard. The supernatant was centrifuged, filtered through a 0.45 μm Millipore filter and transferred to an NMR tube. The ^{1}H NMR spectrum was recorded on a Bruker Advance III HD 800 MHz spectrometer equipped with a 5-mm cryogenic CP-TCI z-gradient probe (Bruker, Fällanden, Switzerland). The spectrum was acquired at 298 K using 90° pulse length. Sixty-four scans were acquired with a time-domain (TD) of 81,088, a spectral width (SW) of 16,025.64 Hz, an acquisition time (AQ) of 2.53 s, and a relaxation delay (D1) of 5 s. The experiment was carried out without water suppression. The spectrum was processed and analyzed using TopSpin 3.6.2 software (Bruker). The spectrum was phased, baseline corrected, and referenced to the TSP peak (0 ppm). The SI-value was 65,536 (zero filling performed), WDW = EM, the line broadening (LB) value was 0.30 Hz. Pulsecal was used to optimize P1. A manual integration of the methanol and acetic acid signals (3.354 ppm for methanol and 1.919 ppm for acetic acid) and comparison with the TSP area was performed in order to quantitatively determine the content of methanol and acetic acid in DMP-AF. The integrals were converted into mass values (mg) according to the formula in Müller-Maatsch et al., 2014. Further, the degree of methylation and acetylation was calculated, using the following equation:

$$degree\ of\ methylation = \frac{mol\ of\ methanol}{mol\ of\ galacturonic\ acid} \times 100\%$$

2.13. Enzyme-linked immunosorbent assay (ELISA)

Human TNF-α or human IFN-γ ELISA were tested using a kit from Mabtech (Sweden) as described previously (Ulriksen et al., 2022). PBMCs (1×10^5 cells/200 μL) were co-cultured in complete medium (RPMI-1640 (ThermoFisher Scientific) supplemented with 10% heat-inactivated fetal bovine serum (Atlanta Biologics), 1 mM Sodium pyruvate, 50 μM 2-Mercaptoethanol and 1× Penicillin/Streptomycin (ThermoFisher Scientific)) in presence of 1000 μg/mL, 100 μg/mL, 10 μg/mL or 1 μg/mL of each sample in 96-well U-bottom plates. Medium alone served as negative control, and 1 μg/mL of Concavilin A (ConA) as positive control. 96-well EIA/RIA Flat Bottom High Binding Plates (Corning) were coated overnight (4 °C) with capture antibodies in PBS. The following day, plates were blocked for 1 h at RT with 200 μL/mL Incubation buffer (PBS with 0.05% Tween-20 and 0.1% BSA). After incubation, the plates were washed and assay standards and supernatans were added to each well and incubated for 2 h at RT. Following incubation, the plates were washed and human TNF-α monoclonal detection antibody (Mabtech) diluted in incubation buffer (1 μg/mL) were added to each well (100 μL/well) before incubating for 1 h. After washing, streptavidin-HRP (Mabtech) was added and plates were incubated for 1

h. After incubation and washing, the plates were developed with TMB substrate for 15 min, and development was stopped by adding 1 M HCl. All washes were done using a BioTek ELx405 plate washer with 0.05% Tween-20 in PBS. Absorbance at 450 nm was measured using a Molecular Devices FlexStation 3 Reader. Data were calculated based on standard curve and presented as concentration of pg/mL cytokines in test samples. All samples were run in duplicates on the same plate and all runs were repeated three times.

3. Results and discussion

3.1. Isolation and purification of polysaccharide fractions

The *Daphne mezereum* polysaccharide fraction (DMP) was obtained after ethanol precipitation of the bark water extract. This resulted in a 3.1% yield (related to dried, pulverized plant material) of a brown precipitate. As illustrated by Fig. 1 and the elution profiles in Fig. 2, two fractions were further isolated after applying DMP to an anion exchange column. A neutral fraction, DMP-NF (Fig. 2A), was obtained after eluting with water and an acidic fraction, DMP-AF (Fig. 2B), after eluting with a NaCl-gradient. Both DMP-NF and DMP-AF were white precipitates with a yield of 3.3% and 49% (related to DMP), respectively. DMP-AF was further treated with pectinase due to GalA being the predominant monosaccharide (Table 1). The enzyme solution was purified by gelfiltration on a Superdex 200 column and led to the isolation of an enzymatically degraded product DMP-ED (Fig. 2C) as a white precipitate with a yield of 2.5% (related to DMP-AF). The relevant fractions that were pooled for each DMP-fraction are between the two vertical lines in Fig. 2A-2C.

Table 1
Monosaccharide composition (mol%) after methanolysis and GC-analysis of polysaccharide containing fractions from *D. mezereum*.

Monosaccharide	DMP	DMP-NF	DMP-AF	DMP-ED
Arabinose (Ara)	6.6	24	2.2	8.2
Rhamnose (Rha)	3.3	6.0	2.2	21
Fucose (Fuc)	3.8	1.7	0.80	3.7
Xylose (Xyl)	1.0	9.9	1.0	2.1
Mannose (Man)	2.1	7.0	0.40	7.3
Galactose (Gal)	7.4	15	6.1	11
Glucose (Glc)	22	25	2.3	5.5
Glucuronic acid (GlcA)	1.9	4.5	0.5	5.4
Galacturonic acid (GalA)	54	7.9	85	36
Total carbohydrate content (%*w*/w)	66	90	82	97

3.2. Molecular weight determination of polysaccharide fractions

Dextran polymers with increasing weight average molecular weights (M_W) were applied to a Superose 6 column in order to make a calibration curve to estimate the M_W of DMP-NF, DMP-AF and DMP-ED. The logarithmic value of the dextran polymers were plotted against the fraction tubes in which they were collected. As illustrated by Fig. 2E, DMP-AF had the highest M_W, followed by DMP-NF, which were calculated to be 484 and 24.5 kDa, respectively. Treating DMP-AF with pectinase (DMP-ED) resulted in a fraction with a M_W of 40.3 kDa, which was expected due to the significant amounts of GalA being released from DMP-AF (Table 1).

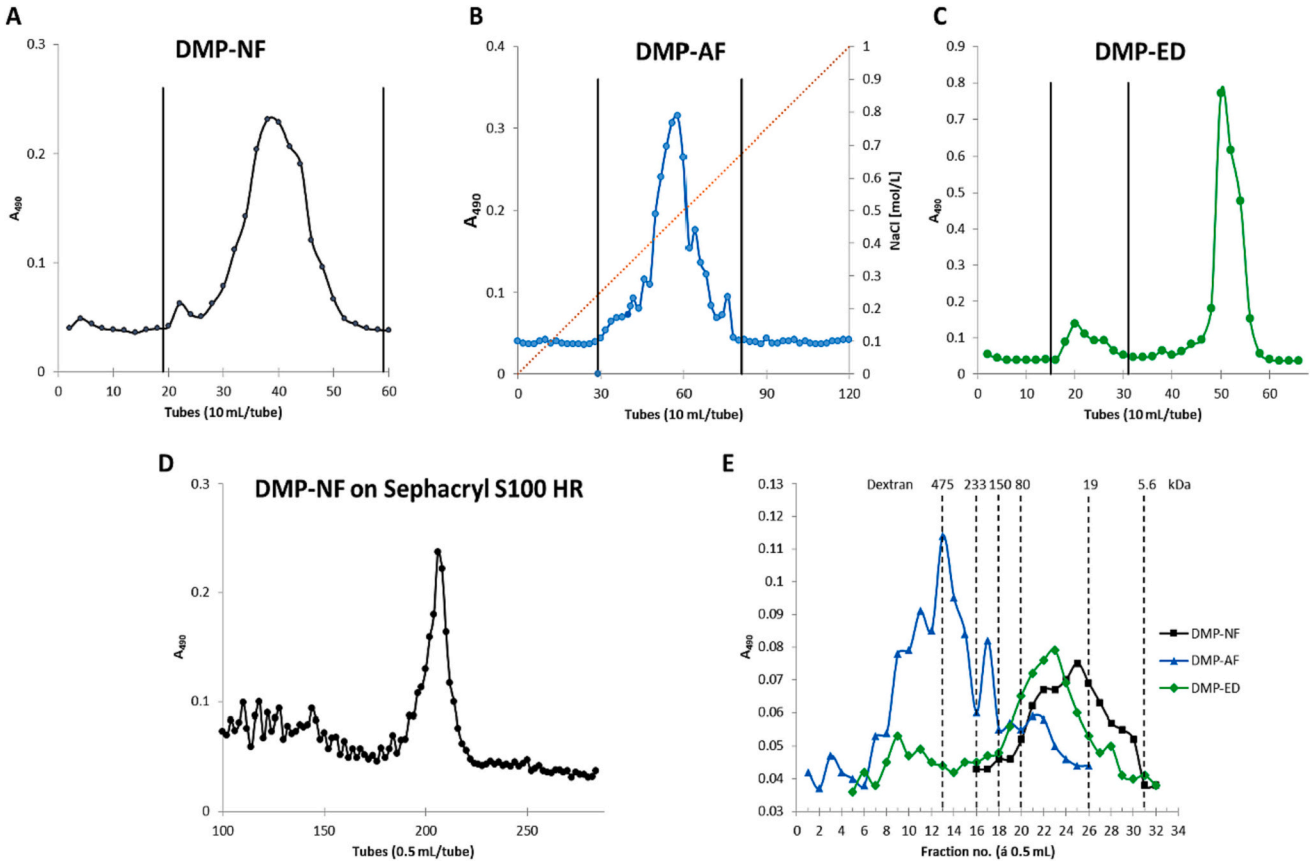

Fig. 2. Elution profiles of the polysaccharide fractions DMP-NF, DMP-AF and DMP-ED isolated from the bark of *D. mezereum*. Anion exchange chromatography elution profiles of DMP-NF (A) and DMP-AF (B) on ANX Sepharose; Size exclusion chromatography elution profiles of DMP-ED (C) on Superdex 200, of DMP-NF on Sephacryl S100 HR (D) and of DMP-NF, DMP-AF and DMP-ED on Superose 6.

3.3. Monosaccharide composition of isolated polysaccharide fractions

The monosaccharide compositions of DMP, DMP-NF, DMP-AF and DMP-ED are given in Table 1. The GC-chromatograms are shown in Fig. S1. In the DMP-fraction, GalA is the most abundant monomer. In addition, noticeable amounts of Ara, Gal and glucose (Glc) were also observed, which could be an early indication of the presence of pectic polymers, hemicellulose and starch. DMP-NF consisted of significant amounts of Ara, Glc and Gal, in addition to xylose (Xyl) and mannose (Man), which could derive from different types of polysaccharides, such as arabinans, arabinogalactans (AG), hemicellulose and starch. Interestingly, minor amounts of GlcA and GalA were also observed in DMP-NF, which could be due to methyl- or acetyl-esterification of the uronic acids, co-eluting with the neutral fractions.

The isolation of DMP-AF yielded a polysaccharide containing relatively high amounts of GalA (85%). Ara, Rha, Gal and Glc were also observable in smaller amounts. This could indicate a pectic polysaccharide with a large HG-domain.

After enzymatically cleaving off GalA in DMP-AF with pectinase, a relative increase of all other monosaccharides in DMP-ED (Table 1) was observed, compared to DMP-AF. In specific, the content of Rha increased significantly, which is probably due to Rha being a part of the backbone in RG-I region of pectins. Ara and Gal were also observed in significant amounts, which could derive from side chains such as arabinans and galactans, or AGs.

3.4. Structural characterization of isolated polysaccharide fractions

3.4.1. Glycosidic linkages

The isolated polysaccharide fractions were analyzed by GC–MS after carboxyl reduction and per-methylation in order to investigate the glycosidic linkages of the monomers. The results are presented in Table 2.

Ara, Glc and Gal were the main monomers detected in DMP-NF. Regarding Ara, the major linkage type observed was 1,5-Ara*f*, in addition to T-, 1,2,5- and 1,3,5-Ara linked units. This suggests a backbone consisting of 1,5-Ara*f* units, with branching occurring at C2 and C3, and could indicate the presence of an arabinan (Mandal et al., 2011). Earlier studies have reported T-Ara*f*, 1,2- and 1,3-Ara*f* residues as possible side chains of arabinans (Xia, Liang, Yang, Wang, & Kuang, 2015). The amount of T-Ara*f* compared to 1,2- and 1,3-Ara*f* insinuate that most of the side chains are mainly monomers of T-Ara*f*.

The main linkage pattern for Glc was 1,4-Glc*p*, which could indicate that DMP-NF contained either starch or hemicellulose. The main difference between the aforementioned polysaccharides is the anomeric configuration. An iodine-starch test can easily distinguish between starch and hemicellulose. Adding a few drops of iodine-solution to DMP-NF and dH_2O (negative control) resulted in a yellow solution, thus asserting the presence of hemicellulose.

Based on the observation above and the linkages observed for mannose and xylose, possible hemicelluloses that may be present are mannans, xylans and xyloglucans. The presence of 1,4- and 1,4,6-Man*p* may derive from mannans which consist of a linear backbone composed entirely of β-1,4-linked Man*p* with branching occurring at O-6. They can be furthered be divided into galactomannan (substituted by single Gal*p* units), glucomannan (backbone consisting of both β-1,4-linked Man*p* and β-1,4-linked Glc*p*) and galactoglucomannan (glucomannan backbone terminated with single Gal*p* units at O-6) (Ebringerová, Hromádková, & Heinze, 2005). Xylans are composed of β-1,4-linked Xyl*p*, and depending on the side chain, can further be divided into glucoronoxylans (Glc*p*A attached to O-2), arabinoxylans (Ara*f* attached to O-2 or/and O-3) or arabinoglucoronxylans (monosubstituted at O-2 and O-3 with Glc*p*A and Ara*f*, respectively) (Ebringerová et al., 2005).

The Gal units were found to be present as 1,4- and 1,3,4-Gal*p* and 1,3-, 1,6-, 1,3,6- and 1,3,4,6-Gal*p*, suggesting that DMP-NF contains both arabinogalactan type-I (AG-I) and type-II (AG-II), respectively. The

Table 2
Glycosidic linkages (mol%) detected by GC–MS analysis in the isolated polysaccharide fractions from *D. mezereum*.

Monosaccharide	Linkage types	R_T [min]	Primary fragments	DMP-NF	DMP-AF	DMP-ED
Ara*f*	T-	12.4	45, 118, 161, 162	5.7	1.4	3.7
	1,2-	14.7	45, 161, 190	0.8	Trace	0.9
	1,3-	14.8	45, 118, 233	0.9	Trace	0.9
	1,5-	15.6	118, 162, 189	10	0.6	2.4
	1,3,5-	17.6	118, 261	3.0	Trace	Trace
	1,2,5-	17.9	129, 130, 189, 190	3.2	Trace	Trace
Rha*p*	T-	13.3	118, 131, 162, 175	0.9	0.7	7.6
	1,2-	15.6	131, 190, 234	4.4	0.6	6.6
	1,3-	15.9	118, 131, 234	Trace	Trace	4.3
	1,2,4-	17.9	190, 203	n.d.	0.6	2.4
Fuc*p*	T-	14.0	118, 131, 162, 175	1.7	0.8	3.7
	1,2,3-	17.7	131, 262	n.d.	Trace	0.6
Xyl*p*	T-	13.3	117, 118, 162	1.9	0.6	0.7
	1,2-	15.7	117, 130, 190	1.3	Trace	0.7
	1,4-	15.7	118, 162, 189	5.2	Trace	0.5
	1,3,4-	17.7	118, 261	1.5	n.d.	Trace
Man*p*-	T-	16.7	45, 118, 161, 162, 205	1.4	Trace	3.0
	1,3-	18.9	118, 161, 234, 277	n.d.	n.d.	n.d.
	1,4-	18.9	45, 118, 162, 233	4.5	Trace	1.1
	1,6-	19.6	118, 162, 189, 233	n.d.	Trace	2.0
	1,2,3-	21.0	161, 262	n.d.	Trace	Trace
	1,4,6-	21.7	118, 162, 261	1.1	Trace	Trace
Gal*f*	T-	16.8	45, 89, 118, 161, 162, 205, 278	0.7	Trace	0.7
	1,3-	18.9	45, 89, 118, 277, 306	Trace	Trace	1.1
Gal*p*	T-	17.2	45, 118, 162, 205	0.6	1.4	1.6
	1,4-	19.0	45, 118, 162, 233	1.7	0.8	1.2
	1,3-	19.4	45, 118, 161, 233	1.3	0.8	1.5
	1,6-	20.4	118, 162, 189, 233	0.6	0.7	1.0
	1,3,4-	20.7	45, 118, 305	2.7	Trace	Trace
	1,2,4-	21.2	45, 130, 190, 233	n.d.	Trace	0.6
	1,4,6-	22.0	118, 162, 261	2.1	n.d.	Trace
	1,3,6-	22.6	118, 189, 234, 305	2.4	2.0	1.6
	1,3,4,6-	23.5	118, 333	1.8	n.d.	Trace
	1,2,3,6-	24.0	189, 262	Trace	n.d.	Trace
Gal*p*A	T-	17.2	47, 118, 162, 207	n.d.	2.0	14
	1,4-	19.0	47, 118, 162, 235	7.9	80.2	14
	1,3,4-	20.8	47, 118, 307	n.d.	1.7	5.5
	1,2,4-	21.2	47, 130, 190, 235	n.d.	0.6	2.6

(*continued on next page*)

Table 2 (*continued*)

Monosaccharide	Linkage types	R_T [min]	Primary fragments	DMP-NF	DMP-AF	DMP-ED
Glc*p*	T-	16.6	45, 118, 161, 162, 205	2.7	Trace	1.9
	1,3-	18.9	45, 118, 161, 234, 277	4.6	n.d.	n.d.
	1,4-	19.2	45, 118, 162, 233	12.3	1.6	1.2
	1,6-	19.6	118, 162, 189, 233	2.6	Trace	1.9
	1,4,6-	21.8	118, 162, 261	2.6	n.d.	0.5
GlcpA	T-	16.6	47, 118, 161, 162, 207	1.6	Trace	3.4
	1,4-	19.2	47, 118, 162, 235	2.9	Trace	2.1

Note: Trace = <0.5 mol%, n.d. = not detected.

presence of the latter was confirmed by the Yariv test. Both AG-domains consist of a Gal-backbone. However, in AG-I the backbone is made up of β-1,4-Gal*p* with branching occurring at O-3, usually with T-Ara*f*, or sometimes even T-Gal. AG-II on the other hand consist of a backbone of β-1,3-Gal*p* with branching occurring at O-6 with β-1,3-Gal*p* or β-1,6-Gal*p* units. The side chains can again be terminated with T-Ara*f* or T-Glc*p*A (Yamada & Kiyohara, 2007).

In an attempt to separate these polysaccharides, DMP-NF was applied to a Sephacryl S-100 column. As seen by Fig. 2D, the separation was not successful. Applying the sample to the Superose 6 column did also not separate them (Fig. 2E). Based on the above, DMP-NF might consist of a mixture of arabinans, arabinogalactans and hemicelluloses with similar M_W. The different parts may also be covalently linked.

The dominant linkage type in DMP-AF was 1,4-linked GalA, as expected for a pectin. However, it accounted for 80% of all linkage types, which is a substantial amount given the fact that 1,4-GalA usually make up around 65% of pectins (Mohnen, 2008). In addition, minor amounts of 1,2,4-linked GalA and traces of 1,3,4-linked GalA were also observed, suggesting a low degree of branching at C-2 or C-3. The remaining monomers were only detected as minor amounts or traces. Presence of T-Xyl*p* may indicate a xylogalacturonan region, in which frequent single Xyl*p*-residues are β-1,3-linked to the Gal-A units (Mort, Zheng, Qiu, Nimtz, & Bell-Eunice, 2008). T-Fuc*p* may also be substituted at C-3 in the HG-region (Fu et al., 2022).

By enzymatically cleaving off the α-1,4-GalA units in DMP-AF by a pectinase, several linkage types were revealed in higher amounts, making it possible to further elucidate the structure of the RG-I region. As for DMP-AF, DMP-ED also contained 1,4- linked Gal*p*A units. In addition 1,2-Rha*p* and 1,2,4-Rha*p* linkages were found, most probably deriving from a RG-I region of the pectin. In addition to arabinan- and AG-II type linkages, 1,4- and 1,3,4-Gal*p* also suggests presence of arabinogalactan-I (AG-I). The 1,4-Gal*p* could also be a part of a linear galactan side chain. The branches may be terminated by T-Ara*f* or arabinans (Mohnen, 2008).

In order to determine the possible presence of RG-II in DMP-ED, a method to determine the amount of 3-deoxy-D-manno-2-octulosonic acid (KDO) was applied (Karkhanis et al., 1978). Both DMP-AF and DMP-ED were subjected to this experiment, in addition to KDO and water as positive and negative control, respectively. Both DMP-AF and DMP-ED tested positive for KDO, thus indicating that both fractions may consist of a RG-II region. This could explain the presence of 1,2,4- and 1,3,4-Gal*p*A, as branching in this region occurs in either O2 or O3, in addition to the presence of T-Rha*p*, 1,3-Rha*p*, 1,2,3-Fuc and T-Gal*p*A (O'Neill, Ishii, Albersheim, & Darvill, 2004). However, further studies should be performed in order to confirm the presence of the RG-II region.

3.4.2. NMR analysis

DMP-NF, DMP-AF and DMP-ED were analyzed by NMR in order to further elucidate their structures. The data were interpreted by comparing and matching chemical shift values from the 1D-spectra ^{1}H (Fig. S2A, S3A and S4A) and ^{13}C (Fig. S2B, S3B and S4B) and the 2D-spectra COSY (Fig. S2C, S3C and S4C), NOESY (Fig. S3D), ROESY (Fig. S2D and S4D), TOCSY (Fig. S2E, S3E and S4E), HSQC (Fig. 3) and HMBC (Fig. 3, Fig. S2F and Fig. S3F). The shift values were assigned to the linkage patterns observed by GC–MS and compared with earlier reported data. The results are presented in Table 3.

The anomeric region in a ^{1}H NMR spectra is defined as peaks occurring in the range between δ 5.6–4.4 (Speciale et al., 2022). It should be noted that some non-anomeric protons can also appear in this region, especially in the upfield part of the region (Yao, Wang, Yin, Nie, & Xie, 2021). Furthermore, the CH_3-group in Rha occur usually in δ 1.1–1.4 in ^{1}H NMR and δ 16–18 region in ^{13}C NMR. Peaks related to acetyl- and methyl groups are encountered in δ 2.0–2.2 and 18–22 and δ 3.3–3.8 and 55–61, respectively (Yao et al., 2021).

3.4.2.1. NMR analysis of DMP-NF. Several peaks and cross peaks were observed around δ 110 in the HSQC spectrum of DMP-NF (Fig. 3A), which can be assigned to the anomeric carbons in the Ara*f*-residues observed in the methylation analysis. For instance, the intense signals at δ 5.15/109.9 (**TA_1–1**), δ 5.19/110.0 (**TA_2–1**) and δ 5.26/112.0 (**TA_3–1**) observed in the HSQC spectra can be assigned to the anomeric carbon of α-Ara*f*-(➔1. The α-Ara*f* residues may differ in terms of their appendences to substituted L-Ara*f* (at O-2, O-3 or O-5) and D-Gal*p* (at O-3 or O-6), hence giving rise to the different proton/carbon signals (H. Zhang et al., 2020). Due to overlapping signals between the H-1 of T-Ara*f* and H-2, H-3 and H-5 of substituted Ara*f* or H-3, H-4 and H-6 of substituted Gal*p*, it was not possible to distinguish between the TA-residues. HMBC (Fig. S2F) revealed cross peaks for H-1 of TA_1 δ 5.15/83.4 (**$H1/C2\text{-}TA_1$**), 5.15/79.5 (**$H1/C3\text{-}TA_1$**) and 5.15/86.9 (**$H1/C4\text{-}TA_1$**) which were assigned to C-2, C-3 and C-4, respectively. Furthermore, H-1 correlated to protons at δ 5.15/3.74 and δ 5.15/3.84 in ROESY (Fig. S2C). The shifts were assigned to the H-5 protons due to the downfield shift of the carbon that the protons are attached to (**TA_1–5**) (Wefers & Bunzel, 2016). The shifts for the remaining TA-residues were also assigned in similar manner.

The H/C correlation at δ 5.09/110.4 (**$A_{1,5}$–1**) in HSQC (Fig. 3A) can be assigned to the C-1 in ➔5)-α-Ara*f*-(1➔. COSY (Fig. S2C) revealed that a cross peak for the anomeric proton at δ 5.09/4.13, which can be appointed to the H-2 (**$A_{1,5}$–2**). Furthermore, the HMBC spectrum (Fig. S2F) showed cross peaks at δ 5.09/79.5 (**$A_{1,5}$–3**) and 5.09/85.2 (**$A_{1,5}$–4**), which can be assigned to C-3 and C-4, respectively. H-5 was deduced by HMBC-correlations (Fig. 3A) at δ 3.89/110.4 (**$A_{1,5}$–5**). Similar approach was also applied when assigning chemical shifts to the branched arabinans (1,2,5- and 1,3,5-Ara*f*). The shifts were in accordance with earlier reported values (Shakhmatov, Makarova, & Belyy, 2019).

Signals correlating to AG-II linkages were also observed. More specifically, H/C correlations at δ 4.63/107.2 (**$G_{1,3}$–1**), δ 4.53/105.8 (**$G_{1,3,6}$–1**) and δ 4.48/106.7 (**$G_{1,3,4,6}$–1**) in HSQC (Fig. 3A) were assigned to the anomeric carbons of ➔3)-β-Gal*p*-(1➔, ➔3,6)-β-Gal*p*-(1➔ and ➔3,4,6)-β-Gal*p*-(1➔, respectively. COSY (Fig. S2C) was used to assign the shift of the H-2 proton and the remaining shifts were assigned using ROESY (Fig. S2D) and TOCSY (Fig. S2E). The assigned shifts were in accordance with earlier reported values (Fu et al., 2022; H. Zhang et al., 2020). COSY (Fig. S2C) also revealed a strong proton-proton coupling at δ 4.63/3.35, which could indicate two overlapping anomeric protons. This was also further confirmed by HMBC cross peak (Fig. 3A) at δ 3.35/105.8 (**$H2/C1\text{-}G^*_{1,4}$**). Given the upfield shift and the intensity of this coupling, the spin system δ 3.35/76.0 (**$G^*_{1,4}$–2**) was assigned to the H-2 of ➔4)-β-Glc*p*-(1➔ residue. ROESY correlations (Fig. S2D) for H-2 at δ 3.35/3.50, 3.35/3.65 and 3.35/3.89 were

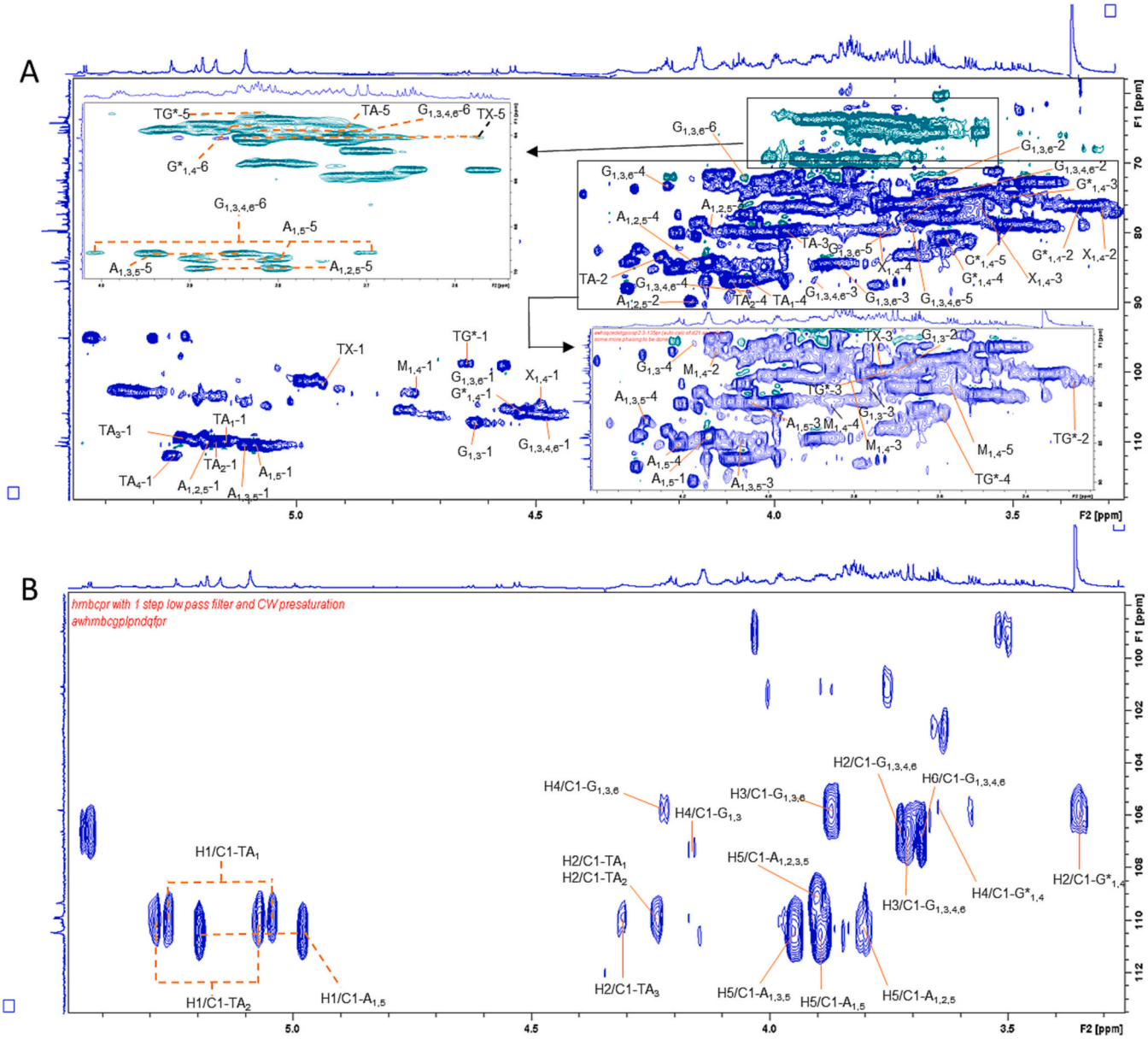

Fig. 3. 2D-NMR with assigned H/C-correlations of DMP-fractions isolated from the bark of *D. mezereum*. HSQC (A) and HMBC (B) spectra of DMP-NF; HSQC (C) and HMBC (D) spectra of DMP-AF and HSQC (E) and HMBC (F) spectra of DMP-ED. Positive signals (blue) are either methine (CH) or methyl (CH_3), while negative signals (green) are methylene (CH_2) groups.

appointed to H-3, H-4 and H-6, respectively. Ultimately, H-5 was deduced by the H-5/C-2 correlation at δ 3.52/76.0 in HMBC (Fig. S2F). This also asserts the results obtained from the iodine-starch test discussed earlier. The shifts belonging to (4➔β-Glc*p* were also determined in similar fashion. The results were in good agreement with published values (Ding et al., 2016; Y. Guo et al., 2023; Makarova & Shakhmatov, 2021).

The presence of ➔4)-β-Man*p*-(1➔ (**$M_{1,4}$**) could also be observed by signals at δ 4.76/103.1 (**$M_{1,4}$–1**) in HSQC (Fig. 3A). The ROESY spectrum (Fig. S2D) revealed cross peaks for H1 at δ 4.76/4.12, 4.76/3.82, 4.75/3.85 and 4.76/3.56, which were assigned to H-2-H-5, respectively. This might suggest the presence of mannans. Moreover, ROESY (Fig. S2D) also revealed *trans*-glycosidic correlation between H-1 of **$M_{1,4}$** and H-4 of **$G^*_{1,4}$** at δ 4.76/3.65, and between H-1 of **$G^*_{1,4}$** and H-4 of **$M_{1,4}$** at δ 4.53/3.56. This might indicate the presence of the repeating disaccharide unit ➔4)-β-Man*p*-(1➔4)-β-Glc*p*-(1➔ found in glucomannans (Makarova & Shakhmatov, 2021).

Both α-Xyl*p*-(1➔ (**TX**) and ➔4)-β-Xyl*p*-(1➔ (**$X_{1,4}$**) could also be confirmed by the anomeric spin systems at δ 4.95/101.6 (TX-1) and δ 4.49/104.5 (**$X_{1,4}$–1**), respectively. The shift for the H-2 proton was assigned using COSY (Fig. S2C). The remaining protons were deduced by correlations in ROESY (Fig. S2D) and TOCSY (Fig. S2E). The presence of these Xyl*p* residues might indicate that DMP-NF also contains xyloglucan and xylans. The results were in accordance with earlier reported values (Ding et al., 2016; Makarova & Shakhmatov, 2021).

3.4.2.2. NMR analysis of DMP-AF. The spectra of DMP-AF were less crowded compared to the other fractions due to DMP-AF mainly consisting of Gal*p*A (85%). The ^{1}H NMR spectra (Fig. S3A) consisted of four intense peak, one less than expected. With the help of the 2D-spectra, it was deduced that the missing signal overlapped with the water signal, and thus suppressed during acquisition of the one dimensional

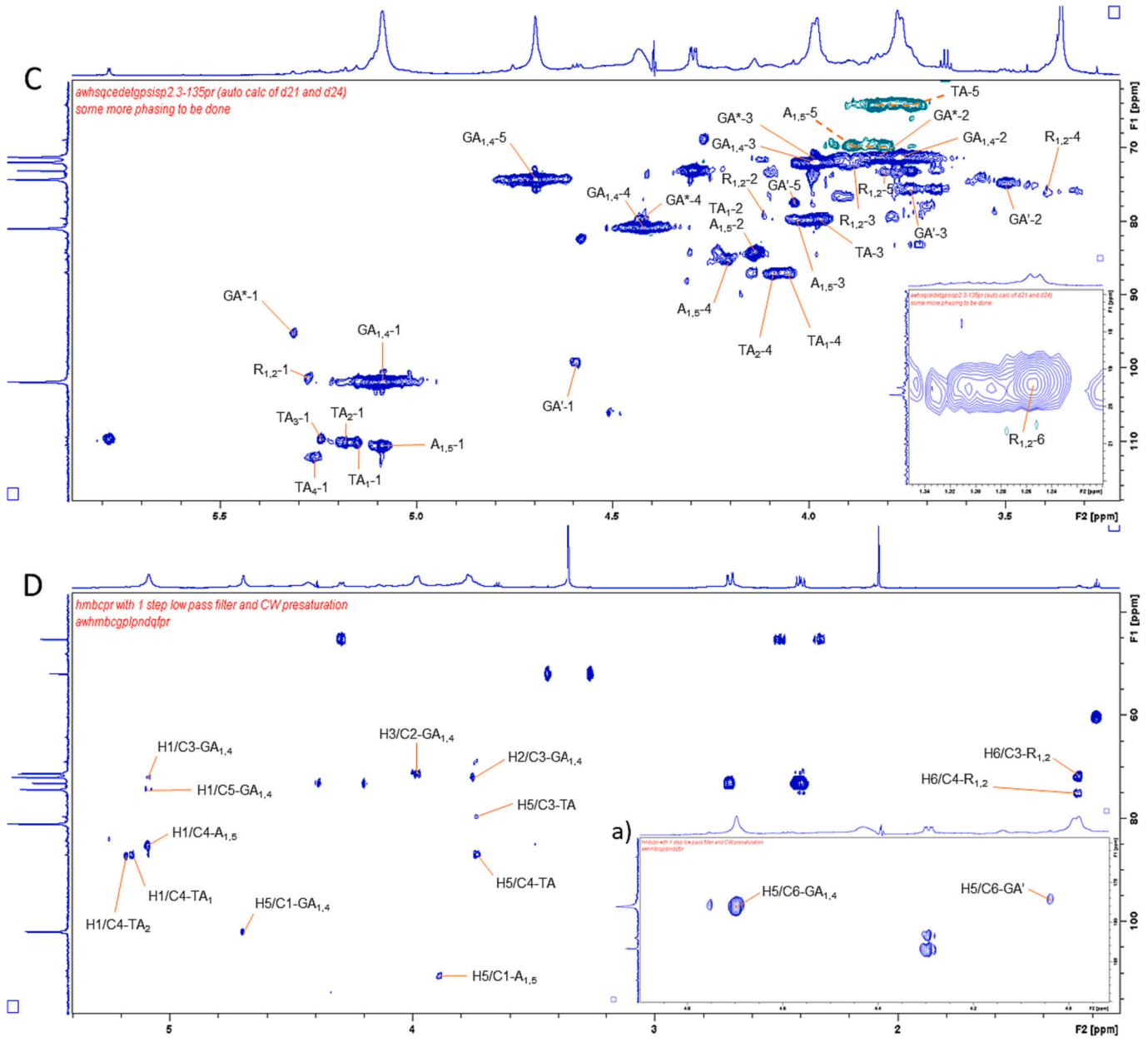

Fig. 3. (*continued*).

spectrum. The H/C-correlation for the intense signal were observed at δ 5.09/101.8 (**GA$_{1,4}$–1**), 3.77/71.2 (**GA$_{1,4}$–2**), 3.98/71.9 (**GA$_{1,4}$–3**), 4.42/81.0 (**GA$_{1,4}$–4**) and 4.70/74.3 (**GA$_{1,4}$–5**) in HSQC (Fig. 3C), which can be assigned to H1/C1-H5/C5 in α-1,4-Gal*p*A in the HG-domain, respectively. The remaining C-6 was deduced by the correlation at δ 4.70/178.0 (**H5/C6-GA$_{1,4}$**) in HMBC (Fig. 3D) (Shakhmatov et al., 2019). The presence of **➔**4)-Gal*p*A residues (**GA*** and **GA'**) were also confirmed. Cross peaks in COSY (Fig. S2C) and TOCSY (Fig. S2E) were used to assign several shifts (e.g. coupling between H-1 and H-2) and C-6 was determined based on HMBC correlations (Fig. 3D). The values were in good agreement with earlier reported values (Fu et al., 2022).

Due to low amounts of the other monosaccharide residues in DMP-AF, the assignment of remaining linkages was significantly more difficult. Nevertheless, the anomeric spin system δ 5.28/101.3 (**R$_{1,2}$–1**) was assigned to α-1,2-Rha*p* (**R$_{1,2}$**) and H-2 was assigned based on the proton-proton coupling observed in COSY (Fig. S3C). The spin system at δ 1.26/19.5 in HSQC (Fig. 3C) was appointed to the C-6 of **R$_{1,2}$** due to its upfield shift. Protons coupling to H-6 at δ 1.26/3.39 and 1.26/3.81 in TOCSY (Fig. S3D) were appointed to H-4 and H-5, respectively. Ultimately, the HMBC spectrum (Fig. 3D) revealed a correlation at δ 1.26/71.8, which was assigned to the remaining C-3. The values were in accordance with reported values from earlier studies (Patova et al., 2019).

3.4.2.3. NMR analysis of DMP-ED. The NMR-spectra of DMP-ED on the other hand was significantly more complicated compared to DMP-AF. In similar manner as discussed above, shifts for the aforementioned linkages were deduced. Furthermore, 1,2,4-α-Rha*p* was identified by the anomeric spin system at δ 5.28/100.9 (**R$_{1,2,4}$–1**). Cross peaks for H-1 at δ 5.28/4.13, 5.28/4.03 and 5.28/3.82 in the ROESY spectrum (Fig. S4D) were allocated to H-2-H-4, respectively. The proton coupling to H-2 at δ 4.12/3.87 in TOCSY (Fig. S4E) was assigned to H-5 and the remaining H-6 was deduced by a strong correlation to C-5 at δ 1.28/71.4 (**H6/C5-R$_{1,2,4}$**) in HMBC (Fig. 3F). The results were in good agreement with earlier reported values (Shakhmatov et al., 2019). In addition, the ROESY spectrum also showed correlation between the H-1 of **R$_{1,2}$** and H-5 of **GA$_{1,4}$**; H-1 of **R$_{1,2}$** and H-4 of **GA$_{1,4}$**, and H-2 of **R$_{1,2}$** and H-1 of

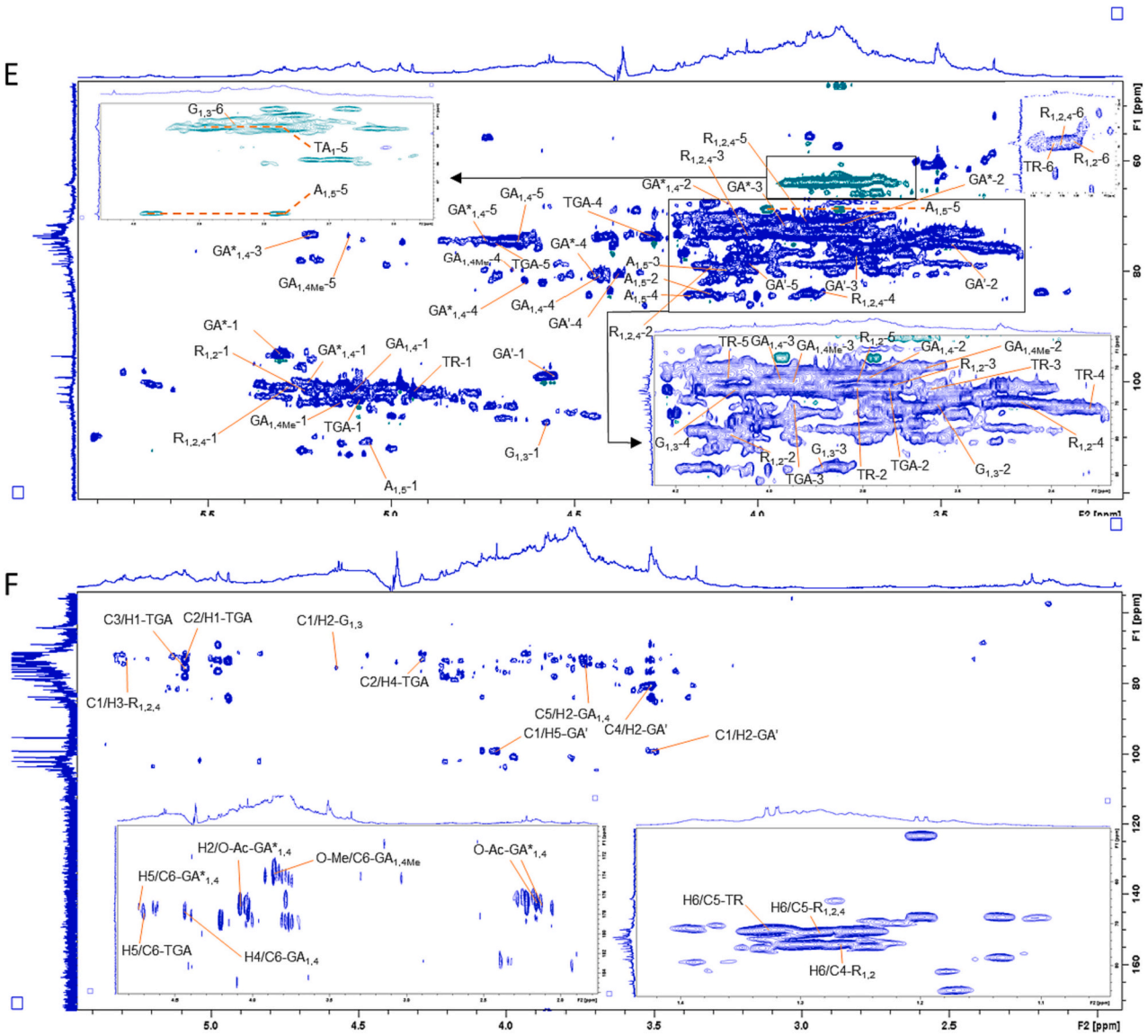

Fig. 3. (*continued*).

GA$_{1,4}$. This confirms the presence of the RG-I backbone moiety ➔4)-α-Gal*p*A-(1➔2)-Rha*p*-(1➔ (Shakhmatov, Belyy, & Makarova, 2018).

In addition to α-1,4-Gal*p*A, cross peaks in the downfield region of the HMBC spectrum suggested the presence of acetylated (**GA*$_{1,4}$**) Gal*p*A. The ➔4)-α-3-O-Ac-Gal*p*A-(1➔ residue was identified by cross peaks at δ 5.23/100.0 (**GA*$_{1,4}$–1**) in HSQC (Fig. 3E), δ 2.15/176.7 (**O-Ac-GA*$_{1,4}$**), 2.16/176.7 (**O-Ac-GA*$_{1,4}$**), 4.08/176.7 (**H2/O-Ac-GA*$_{1,4}$**) and 4.74/177.2 (**H5/C6-GA*$_{1,4}$**) in HMBC (Fig. 3F), and δ 2.15/5.22, 2.16/5.22 and 4.64/5.23 in ROESY (Fig. S4D). The correlation at δ 5.15/103.3, 5.12/73.3 and 3.86/55.4 in HSQC (Fig. 3E) and δ 3.86/173.8 in HMBC (Fig. 3F), in addition to δ 5.15/3.63 in COSY (Fig. S4C) and, δ 3.95/5.15 and 3.95/4.67 in ROESY (Fig. S4D), indicated that some of the α-1,4-Gal*p*A was also methyl-esterified (Patova et al., 2019; Patova et al., 2021).

Based on the NMR-spectra presented in this study, it appears that DMP-NF is composed of a mixture of arabinans, AG-II, xyloglucans, xylans and mannans, while DMP-AF consisted of a pectic polysaccharide with an unusually long HG-backbone. After cleaving of the HG-backbone with pectinase, DMP-ED revealed a RG-I backbone with arabinan, galactan and AGs as side chains. However, due to weak correlations in NMR, it was not possible to determine how the side chains were connected to the RG-I backbone. To our knowledge, this study is the first to isolate and study the structure of the polysaccharides from the Daphne genus.

3.4.3. Degree of methylation (DM) and acetylation (DAc)

An important structural characteristic of homogalacturonan regions in pectin is esterification of the GalA residues with methanol and/or acetic acid. The DM corresponds to the percentage of carboxyl groups that are esterified with methanol, while the degree of acetylation (DAc) is the percentage of GalA units being esterified with one acetyl group (Voragen, Thibault, Axelos, Renard, & Pilnik, 1995). To determine the DM and DAc of the homogalacturonan in DMP-AF an ^{1}H NMR method was performed as described by Müller-Maatsch et al., 2014. The ^{1}H NMR spectrum of DMP-AF is shown in Fig. 4. The DM and DAc of the GalA residues were calculated based on the content of methanol and acetic acid, and the content of GalA. The content of GalA (mol%) was determined by methanolysis, followed by GC. Based on the calculations it was shown that the DM and DAc in DMP-AF was 22.9%, and 1.8%, respectively. This is in accordance with the literature where methyl-esterification is regarded to be common for pectins, while acetyl-esterification is usually low (Levigne, Thomas, Ralet, Quemener, & Thibault, 2002). Further, pectins are usually classified as low DM pectins (DM < 50%) or high DM pectins (DM > 50%), and based on this DMP-AF

Table 3
NMR chemical shift assignment of DMP-NF, DMP-AF and DMP-ED. The spectra were recorded at 60 °C in D_2O.

Residues (Abb.)	Abb.	H1/C1	H2/C2	H3/C3	H4/C4	H5/C5	H6/C6	O-Me/O-$\underline{C}H_3$	O-Ac/$\underline{C}H_3CO$ ($CH_3\underline{C}O$)
DMP-NF									
α-Ara*f*-(1➔	(TA_1)	5.15/ 109.9	4.24/ 83.4	3.98/ 79.5	4.06/ 86.9	3.74, 3.84/64.1			
	(TA_2)	5.18/ 110.0	4.24/ 83.4	3.98/ 79.5	4.09/ 87.1	3.74, 3.82/64.0			
	(TA_3)	5.25/ 109.3	4.30/ 84.0		4.09	3.81, 3.89/n.d.			
	(TA_4)	5.26/ 112.0	4.34/ 87.0						
➔5)-α-Ara*f*-(1➔	($A_{1,5}$)	5.09/ 110.4	4.13/ 84.2	4.04/ 79.7	4.21/ 85.2	3.81, 3.89/69.4			
➔2,5)-α-Ara*f*-(1➔	($A_{1,2,5}$)	5.19/ 109.9	4.17/ 89.8	4.14/ 79.7	4.16/ 84.3	3.81, 3.88/69.9			
➔3,5)-α-Ara*f*-(1➔	($A_{1,3,5}$)	5.11/ 110.4	4.11/n.d.	4.06/ 84.5	4.29/ 82.2	3.85, 3.94/69.2			
➔3)-β-Gal*p*-(1➔	($G_{1,3}$)	4.63/ 107.2	3.71/ 75.8	3.81/ 84.3	4.17/ 72.2	n.d.	3.78/63.8		
➔3,6)-β-Gal*p*-(1➔	($G_{1,3,6}$)	4.53/ 105.8	3.64/ 74.5	3.87/ 84.3	4.22/ 73.1	3.67/75.6	n.d., 4.06/72.0		
➔3,4,6)-β-Gal*p*-(1➔	($G_{1,3,4,6}$)	4.48/ 106.7	3.72/ 75.7	3.92/ 86.9	4.05/ 88.5	3.71/ 79.3	3.68, 4.00/69.1		
➔4)-β-Glc*p*	(TG*)	4.65/ 98.7	3.29/ 77.0	3.77/ 75.8	3.60/ 81.1	n.d.	3.81, 3.88/63.6		
➔4)-β-Glc*p*-(1➔	($G^*_{1,4}$)	4.53/ 105.8	3.35/ 76.0	3.50/ 74.8	3.65/ 80.4	3.52/78.6	3.81, 3.89/63.6		
➔4)-β-Man*p*-(1➔	($M_{1,4}$)	4.76/ 103.1	4.12/ 73.0	3.82/ 76.1	3.85/ 80.2	3.56/78.0	n.d.		
α-Xyl*p*-(1➔	(TX)	4.95/ 101.6	3.55/n.d	3.73/ 75.7	n.d.	3.56, 3.76/63.9			
➔4)-β-Xyl*p* -(1➔	($X_{1,4}$)	4.49/ 104.5	3.32/ 75.9	3.58/ 75.5	3.78/ 79.4	3.32, 4.00/n.d			
DMP-AF									
α-Ara*f*-(1➔	(TA_1)	5.16/ 110.0	4.14/ 84.0	3.97/ 79.5	4.05/ 87.0	3.73, 3.83/64.1			
	(TA_2)	5.18/ 110.0	4.14/ 84.0	3.97/ 79.5	4.09/ 87.0	3.74, 3.83/64.1			
	(TA_3)	5.24/ 109.5	3.99/n.d.						
	(TA_4)	5.26/ 112.1							
5➔)-α-Ara*f*-(1➔	($A_{1,5}$)	5.09/ 110.4	4.14/ 84.0	4.02/ 79.8	4.21/ 85.2	3.81, 3.89/69.7			
➔4)-α-Gal*p*A-(1➔	($GA_{1,4}$)	5.09/ 101.8	3.77/ 71.2	3.98/ 71.9	4.42/ 81.0	4.70/74.3	–/178.0		
➔4)-α-Gal*p*A	(GA*)	5.31/ 95.1	3.83/ 71.2	3.99/ 71.5	4.43/ 79.7	n.d.	n.d.		
➔4)-β-Gal*p*A	(GA')	4.60/ 99.1	3.50/ 74.7	3.74/ 75.4	4.27/n.d.	4.04/77.4	–/177.2		
➔2)-α-Rha*p*-(1➔	($R_{1,2}$)	5.28/ 101.3	4.11/ 79.3	3.89/ 71.8	3.39/ 75.5	3.81/73.3	1.26/19.5		
DMP-ED									
α-Ara*f*-(1➔	(TA_1)	5.24/ 112.1	4.13/ 83.9	n.d.	4.02/ 86.0	3.77, 3.88/63.7			
	(TA_2)	5.12/ 113.0	4.15/ 84.2						
	(TA_3)	5.14/ 113.0							
5➔)α-Ara*f*-(1➔	($A_{1,5}$)	5.06/ 110.6	4.13/ 83.9	4.08/ 79.4	4.18/ 84.1	3.78, 3.97/68.7			
➔3)-β-Gal*p*-(1➔	($G_{1,3}$)	4.58/ 107.2	3.64/ 75.2	3.88/ 84.1	4.07/ 73.0	n.d.	3.85/63.8		
α-Gal*p*A-(1➔	(TGA)	5.09/ 103.2	3.74/ 72.9	3.95/ 75.2	4.28/ 73.5	4.71/74.3	–/177.9		
➔4)-α-Gal*p*A	(GA*)	5.30/ 95.1	3.83/ 71.3	3.99/ 72.0	4.45/ 80.7	n.d.	n.d.		
➔4)-β-Gal*p*A	(GA')	4.57/ 98.8	3.52/ 74.6	3.73/ 76.1	4.38/ 80.3	4.03/78.3	–/177.0		
		4.58/ 98.9	3.49/ 74.6						
➔4)-α-Gal*p*A-(1➔	($GA_{1,4}$)	5.12/ 101.9	3.79/ 71.2	3.98/ 71.9	4.44/ 81.0	4.66/74.2	–/177.7		

(*continued on next page*)

Table 3 (*continued*)

Residues (Abb.)	Abb.	H1/C1	H2/C2	H3/C3	H4/C4	H5/C5	H6/C6	O-Me/O-$\underline{C}H_3$	O-Ac/$\underline{C}H_3CO$ ($CH_3\underline{C}O$)
→4)-α-3-O-Ac-Galp*A*-(1→	($GA^*_{1,4}$)	5.23/ 100.0	4.08/ 67.4	5.22/ 73.2	4.64/ 81.5	4.74/74.1	–/177.2		2.16/23.1 2.15/23.1 (176.7)
→4)-α-GalpA-6-*O*-Me-(1→	($GA_{1,4Me}$)	5.15/ 103.3	3.63/ 69.6	3.95/ 72.2	4.67/ 79.6	5.12/73.3	–/173.8	3.86/55.4	
α-Rhap-(1→	(TR)	4.94/ 101.8	3.81/ 72.9	3.66/ 72.9	3.32/ 75.7	4.09/71.3	1.33/19.7		
→2)-α-Rhap-(1→	($R_{1,2}$)	5.23/ 101.4	4.08/ 79.4	3.95/ 72.7	3.46/ 74.8	3.81/72.0	1.26/19.5		
→2,4)-α-Rhap-(1→	($R_{1,2,4}$)	5.28/ 100.9	4.13/ 79.0	4.03/ 72.9	3.82/ 83.7	3.87/72.0	1.28/19.6		

Note: Abb = Abbreviation, n.d. = not detected.

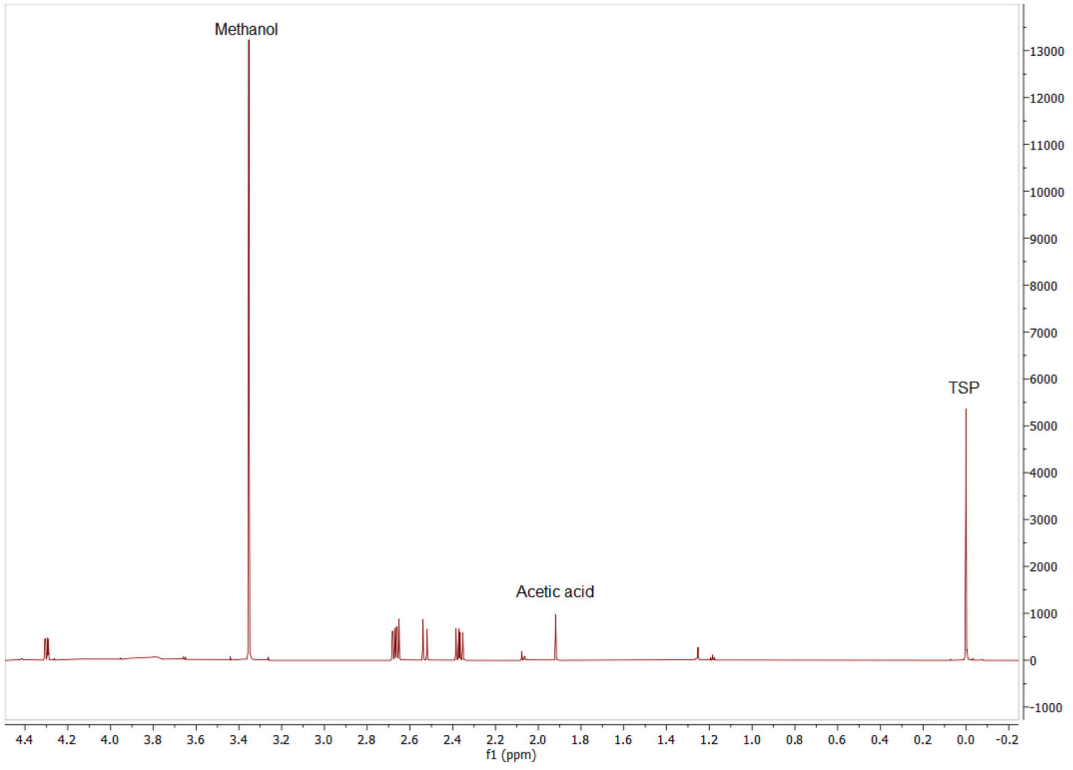

Fig. 4. ^{1}H NMR spectrum of DMP-AF. The signals of methanol and acetic acid are found at 3.354 ppm and 1.919 ppm, respectively. TSP is used as internal standard.

is considered a low DM pectin (Beukema, Faas, & de Vos, 2020).

3.4.4. *Immune-activating effects of DMP-fractions*

To assess the immune activating effect of the DMP-fractions, secretions of TNF-α and IFN-γ from PBMCs were analyzed. Previous studies indicates that pectic arabinogalactans can activate immune cells by recognizing and binding to specific PRRs, such as TLR4, TLR2 and CD-19 (Nergard et al., 2005). This can then lead to the transcriptional activation and production of inflammation-related cytokines (Yin, Zhang, & Li, 2019). The receptors may work separately or cooperate with other receptors by forming clusters of signaling complexes.

As illustrated in Fig. 5, DMP-AF exhibited significantly lower effect in inducing cytokine secretion from PBMCs compared to the other DMP-fractions. Given the fact that the HG-domain is a substantial part of DMP-AF, the lower bioactivity observed may be due to the presence of uncommonly high amounts of GalA residues (85%). By enzymatically cleaving of the 1,4-linked GalA in DMP-AF, DMP-ED was isolated and a significant increase in cytokine secretion was observed. Based on previous studies, there may be several possibilities which could explain the difference in bioactivity. For instance, a previous study looking at how the content of GalA in pectins affect immunomodulatory activity, reported a decrease in macrophage activity of pectins containing GalA residues >80% (Popov & Ovodov, 2013). These results could suggest a possible relationship between the GalA content in pectins and macrophage activity. Further, the DM of pectins is thought to influence their immune activating effects, but so far there is no clear evidence whether low or high DM is most active (Beukema et al., 2020). DMP-AF was found to be a low DM pectin.

A further possible explanation might be that the RG-I region becomes more sterically accessible to interact with PRRs on immune cells. Studies on pectic polysaccharide with a RG-I enriched domain, have reported promising immunostimulatory effects on PBMCs (McKay et al., 2021; Santos et al., 2021). The RG-I region consist of neutral side chains consisting mainly of Ara and Gal. Removal of these side chains have shown to significantly reduce the bioactivity in previous studies (do Nascimento, Winnischofer, Ramirez, Iacomini, & Cordeiro, 2017; Ho et al., 2015), thus indicating that they might play an important role for the bioactivity observed.

DMP-NF exhibited similar levels of cytokine secretion as DMP-ED at the highest concentrations. Due to the high amounts of Ara and Gal

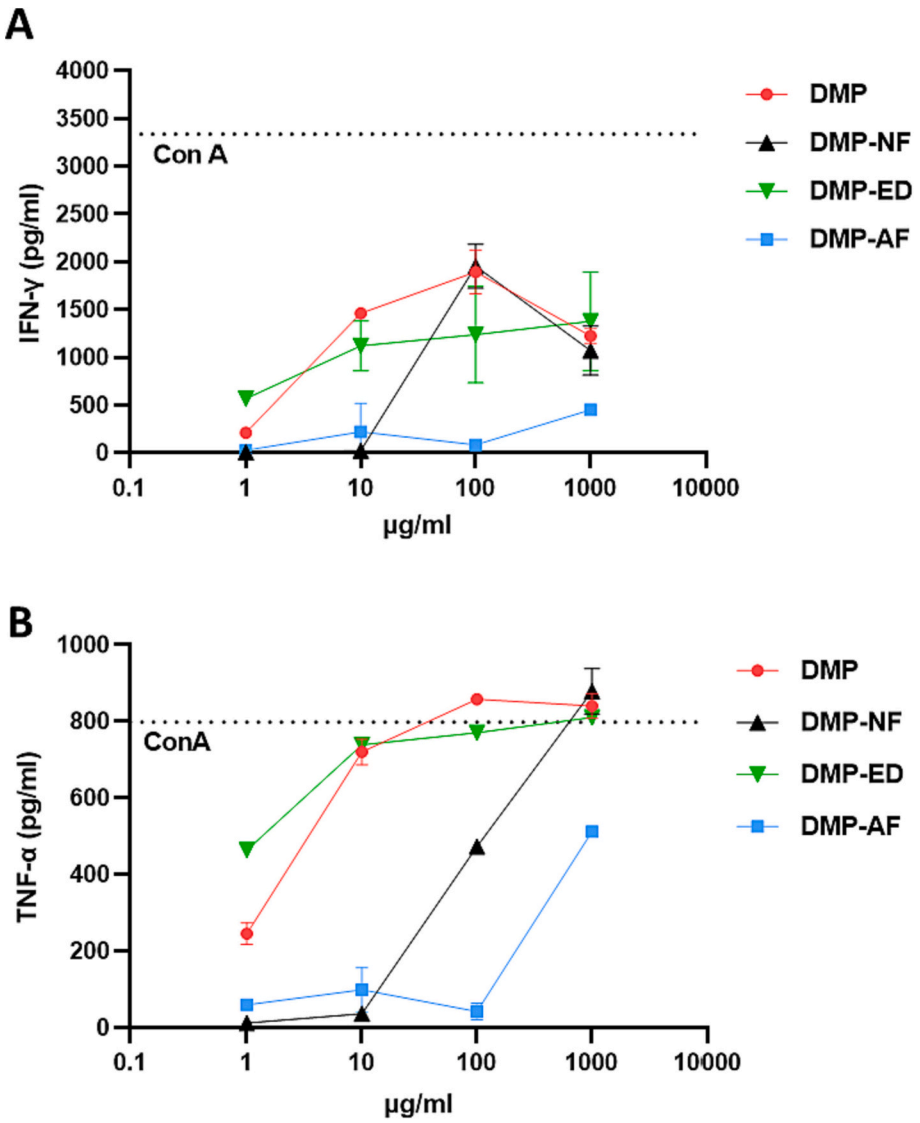

Fig. 5. IFN-γ (A) and TNF-α (B) secretion in supernatants from overnight cultures of PBMCs with DMP-fractions measured via ELISA. Data are presented as pg/mL and calculated based on a standard curve.

observed, it is likely that polysaccharides containing the aforementioned monosaccharides play a role in the bioactivity exhibited by the fractions. However, Glc was also observed in significant amounts (mainly β-1,4-linked), suggesting the presence of hemicellulose. Previous studies have shown that hemicellulose, such as acetylated glucomannan and xyloglucans, can possess immunomodulating activity (Guo et al., 2022; Košťálová, Hromádková, Paulsen Berit, & Ebringerová, 2014). Another explanation may also be a synergistic effect of the different polysaccharides found in DMP-NF. Nevertheless, further isolation is required in order to determine this. Furthermore, a more comprehensive structure-bioactivity relationship study should be performed on the polysaccharide fractions in order to get a better understanding of what part of the polysaccharide fractions is responsible for the promising pro-inflammatory activity.

4. Conclusion

The present study is the first to report a comprehensive structural characterization of the polysaccharides in the Daphne genus. From a water extract of the bark of *D. mezereum*, a neutral fraction (DMP-NF) and an acidic fraction (DMP-AF) were isolated. The latter was further enzymatically degraded with pectinase, which led to the sub-fraction DMP-ED. DMP-NF appeared to be a mixture of several polysaccharides such as arabinans, xyloglucans, xylans and mannans. The combination of GalA, Rha and Gal in DMP-AF suggests the presence of a pectic polysaccharide. The significant amounts of GalA, the α-1,4-linked Gal*p*A in particular, points to a predominant HG-domain. DMP-ED contained a more isolated RG-I backbone with arabinan, galactan and arabinogalactan as side chains. The levels of TNF-α and IFN-γ secreted by PBMCs after stimulation with DMP-NF and DMP-ED indicated potent immune-activating properties of these two fractions, that were significantly higher than that of DMP-AF. Aspects such as GalA-content, molecular weight and steric accessibility of RG-I backbone may be some of the reasons for the difference observed in the bioactivity. This study does not only show the diversity of polysaccharide that may be found in *D. mezereum*, but also their potential as immunomodulators.

CRediT authorship contribution statement

Hussain Shakeel Butt: Investigation, Methodology, Data curation, Visualization, Writing – original draft. **Emilie Steinbakk Ulriksen:** Investigation, Methodology, Data curation, Visualization, Writing – review & editing. **Frode Rise:** Methodology, Software, Writing – review & editing. **Helle Wangensteen:** Supervision, Project administration,

Writing – review & editing. **Jens Øllgaard Duus:** Data curation, Supervision, Writing – review & editing. **Marit Inngjerdingen:** Methodology, Resources, Writing – review & editing. **Kari Tvete Inngjerdingen:** Methodology, Supervision, Project administration, Writing – review & editing.

Declaration of competing interest

The authors declare that they have no known competing financial interests or personal relationships that could have appeared to influence the work reported in this paper.

Data availability

Data will be made available on request.

Acknowledgement

This work was conducted through the convergence environment REA:Life. Convergence environments are interdisciplinary research groups that aim to solve grand challenges related to health and environment, and are funded by the University of Oslo's interdisciplinary strategic area UiO:Life Science. The first author also acknowledges the help from Suthajini Yogarajah and Anne Grethe Hamre for technical assistance. This work was partly supported by the Research Council of Norway through the Norwegian NMR Platform, NNP (226244/F50).

Appendix A. Supplementary data

Supplementary data to this article can be found online at https://doi.org/10.1016/j.carbpol.2023.121554.

References

Beukema, M., Faas, M. M., & de Vos, P. (2020). The effects of different dietary fiber pectin structures on the gastrointestinal immune barrier: Impact via gut microbiota and direct effects on immune cells. *Expermiental & Molecular Medicine, 52*, 1364–1376.

Bonnin, E., Garnier, C., & Ralet, M.-C. (2014). Pectin-modifying enzymes and pectin-derived materials: Applications and impacts. *Applied Microbiology and Biotechnology, 98*(2), 519–532.

Chambers, R. E., & Clamp, J. R. (1971). An assessment of methanolysis and other factors used in the analysis of carbohydrate-containing materials. *Biochemical Journal, 125*(4), 1009–1018.

Ding, H. H., Cui, S. W., Goff, H. D., Chen, J., Guo, Q., & Wang, Q. (2016). Xyloglucans from flaxseed kernel cell wall: Structural and conformational characterisation. *Carbohydrate Polymers, 151*, 538–545.

do Nascimento, G. E., Winnischofer, S. M. B., Ramirez, M. I., Iacomini, M., & Cordeiro, L. M. C. (2017). The influence of sweet pepper pectin structural characteristics on cytokine secretion by THP-1 macrophages. *Food Research International, 102*, 588–594.

DuBois, M., Gilles, K. A., Hamilton, J. K., Rebers, P. A., & Smith, F. (1956). Colorimetric method for determination of sugars and related substances. *Analytical Chemistry, 28*(3), 350–356.

Ebringerová, A., Hromádková, Z., & Heinze, T. (2005). Hemicellulose. In T. Heinze (Ed.), Polysaccharides I: Structure, characterization and use (pp. 1–67). Berlin, Heidelberg: Springer Berlin Heidelberg.

Fu, Y.-P., Li, C.-Y., Peng, X., Zou, Y.-F., Rise, F., Paulsen, B. S., … Inngjerdingen, K. T. (2022). Polysaccharides from *Aconitum carmichaelii* leaves: Structure, immunomodulatory and anti-inflammatory activities. *Carbohydrate Polymers, 291*, Article 119655.

Gao, X., Qi, J., Ho, C.-T., Li, B., Mu, J., Zhang, Y., Hu, H., Mo, W., Chen, Z., & Xie, Y. (2020). Structural characterization and immunomodulatory activity of a water-soluble polysaccharide from *Ganoderma leucocontextum* fruiting bodies. *Carbohydrate Polymers, 249*, Article 116874.

Görick, C., & Melzig, M. F. (2013). Gniditrin is the main diterpenoid constituent in the bark of *Daphne mezereum* L. *Pharmazie, 68*(7), 640–642.

Guo, X., Yang, M., Wang, C., Nie, S., Cui, S. W., & Guo, Q. (2022). Acetyl-glucomannan from Dendrobium officinale: Structural modification and immunomodulatory activities. *Frontiers in Nutrition, 9*.

Guo, Y., Zhang, Z., Dou, J., Liu, G., Li, X., & Zhao, J. (2023). Structural characterization of corn fiber hemicelluloses extracted by organic solvent and screening of degradation enzymes. *Carbohydrate Polymers, 313*, Article 120820.

Ho, G. T. T., Ahmed, A., Zou, Y.-F., Aslaksen, T., Wangensteen, H., & Barsett, H. (2015). Structure–activity relationship of immunomodulating pectins from elderberries. *Carbohydrate Polymers, 125*, 314–322.

Høeg, O. A. (1974). *Planter og tradisjon: Universitetsforl*.

Huang, G., Chen, F., Yang, W., & Huang, H. (2021). Preparation, deproteinization and comparison of bioactive polysaccharides. *Trends in Food Science & Technology, 109*, 564–568.

Huang, L., Zhao, J., Wei, Y., Yu, G., Li, F., & Li, Q. (2021). Structural characterization and mechanisms of macrophage immunomodulatory activity of a pectic polysaccharide from *Cucurbita moschata* Duch. *Carbohydrate Polymers, 269*, Article 118288.

Hunter, R. A., McIntyre, B. L., & McIlroy, R. J. (1970). Water-soluble carbohydrates of tropical pasture grasses and legumes. *Journal of the Science of Food and Agriculture, 21*(8), 400–405.

Karkhanis, Y. D., Zeltner, J. Y., Jackson, J. J., & Carlo, D. J. (1978). A new and improved microassay to determine 2-keto-3-deoxyoctonate in lipopolysaccharide of gram-negative bacteria. *Analytical Biochemistry, 85*(2), 595–601.

Koropatkin, N. M., Cameron, E. A., & Martens, E. C. (2012). How glycan metabolism shapes the human gut microbiota. *Nature Reviews Microbiology, 10*(5), 323–335.

Košťálová, Z., Hromádková, Z., Paulsen Berit, S., & Ebringerová, A. (2014). Bioactive hemicelluloses alkali-extracted from *Fallopia sachalinensis* leaves. *Carbohydrate Research, 398*, 19–24.

Kreher, B., Wagner, H., & Neszmélyi, A. (1990). Triumbellin, A tricoumarin rhamnopyranoside from Daphne mezereum. *Phytochemistry, 29*(11), 3633–3637.

Kupchan, S. M., & Baxter, R. L. (1975). Mezerein: Antileukemic principle isolated from *Daphne mezereum* L. *Science, 187*(4177), 652–653.

Levigne, S., Thomas, M., Ralet, M.-C., Quemener, B., & Thibault, J.-F. (2002). Determination of the degrees of methylation and acetylation of pectins using a C18 column and internal standards. *Food Hydrocolloids, 16*, 547–550.

Makarova, E. N., & Shakhmatov, E. G. (2021). Characterization of pectin-xylan-glucan-arabinogalactan proteins complex from Siberian fir *Abies sibirica* Ledeb. *Carbohydrate Polymers, 260*, Article 117825.

Mandal, S., Patra, S., Dey, B., Bhunia, S. K., Maity, K. K., & Islam, S. S. (2011). Structural analysis of an arabinan isolated from alkaline extract of the endosperm of seeds of *Caesalpinia bonduc* (Nata Karanja). *Carbohydrate Polymers, 84*(1), 471–476.

Maxwell, E. G., Belshaw, N. J., Waldron, K. W., & Morris, V. J. (2012). Pectin – An emerging new bioactive food polysaccharide. *Trends in Food Science & Technology, 24*(2), 64–73.

McKay, S., Oranje, P., Helin, J., Koek, J. H., Kreijveld, E., van den Abbeele, P., … Albers, R. (2021). Development of an affordable, sustainable and efficacious plant-based immunomodulatory food ingredient based on bell pepper or carrot RG-I Pectic polysaccharides. *Nutrients, 13*(3).

Mohnen, D. (2008). Pectin structure and biosynthesis. *Current Opinion in Plant Biology, 11*(3), 266–277.

Moon, C. K., Park, K. S., Lee, S. H., & Yoon, Y. P. (1985). Antitumor activities of several phytopolysaccharides. *Archives of Pharmacal Research, 8*(1), 42–44.

Mort, A., Zheng, Y., Qiu, F., Nimtz, M., & Bell-Eunice, G. (2008). Structure of xylogalacturonan fragments from watermelon cell-wall pectin. Endopolygalacturonase can accommodate a xylosyl residue on the galacturonic acid just following the hydrolysis site. *Carbohydrate Research, 343*(7), 1212–1221.

Moshiashvili, G., Tabatadze, N., & Mshvildadze, V. (2020). The genus Daphne: A review of its traditional uses, phytochemistry and pharmacology. *Fitoterapia, 143*, Article 104540.

Müller-Maatsch, J., Caligiani, A., Tedeschi, T., Elst, K., & Sforza, S. (2014). Simple and validated quantitative ^{1}H NMR method for the determination of methylation, acetylation, and feruloylation degree of pectin. *Journal of Agricultural and Food Chemistry, 62*, 9081–9087.

Nergard, C. S., Matsumoto, T., Inngjerdingen, M., Inngjerdingen, K., Hokputsa, S., Harding, S. E., … Yamada, H. (2005). Structural and immunological studies of a pectin and a pectic arabinogalactan from Vernonia kotschyana Sch. Bip. ex Walp. (Asteraceae). *Carbohydrate Research, 340*(1), 115–130.

O'Neill, M. A., Ishii, T., Albersheim, P., & Darvill, A. G. (2004). Rhamnogalacturonan II: Structure and function of a borate cross-linked cell wall pectic polysaccharide. *Annual Review of Plant Biology, 55*(1), 109–139.

Patova, O. A., Luanda, A., Paderin, N. M., Popov, S. V., Makangara, J. J., Kuznetsov, S. P., & Kalmykova, E. N. (2021). Xylogalacturonan-enriched pectin from the fruit pulp of *Adansonia digitata*: Structural characterization and antidepressant-like effect. *Carbohydrate Polymers, 262*, Article 117946.

Patova, O. A., Smirnov, V. V., Golovchenko, V. V., Vityazev, F. V., Shashkov, A. S., & Popov, S. V. (2019). Structural, rheological and antioxidant properties of pectins from *Equisetum arvense* L. and *Equisetum sylvaticum* L. *Carbohydrate Polymers, 209*, 239–249.

Pettolino, F. A., Walsh, C., Fincher, G. B., & Bacic, A. (2012). Determining the polysaccharide composition of plant cell walls. *Nature Protocols, 7*(9), 1590–1607.

Popov, S. V., & Ovodov, Y. S. (2013). Polypotency of the immunomodulatory effect of pectins. *Biochemistry (Moscow), 78*(7), 823–835.

Prado, S. B. R., Beukema, M., Jermendi, E., Schols, H. A., de Vos, P., & Fabi, J. P. (2020). Pectin interaction with immune receptors is modulated by ripening process in papayas. *Scientific Reports, 10*(1), 1690.

Sahasrabudhe, N. M., Beukema, M., Tian, L., Troost, B., Scholte, J., Bruininx, E., … de Vos, P. (2018). Dietary fiber pectin directly blocks toll-like receptor 2–1 and prevents doxorubicin-induced ileitis. *Frontiers in Immunology, 9*.

Santos, D. K. D.d. N., Barros, B. R. D. S., Filho, I. J. D. C., Júnior, N. D. S. B., Da Silva, P. R., Nascimento, P. H. D. B., … De Melo, C. M. L. (2021). Pectin-like polysaccharide extracted from the leaves of *Conocarpus erectus* Linnaeus promotes antioxidant, immunomodulatory and prebiotic effects. *Bioactive Carbohydrates and Dietary Fibre, 26*, Article 100263.

Shakhmatov, E. G., Belyy, V. A., & Makarova, E. N. (2018). Structure of acid-extractable polysaccharides of tree greenery of *Picea abies*. *Carbohydrate Polymers, 199*, 320–330.

Shakhmatov, E. G., Makarova, E. N., & Belyy, V. A. (2019). Structural studies of biologically active pectin-containing polysaccharides of pomegranate *Punica granatum*. *International Journal of Biological Macromolecules, 122*, 29–36.

Siddiqui, M. T., & Cresci, G. A. M. (2021). The immunomodulatory functions of butyrate. *Journal of Inflammation Research, 14*, 6025–6041.

Speciale, I., Notaro, A., Garcia-Vello, P., Di Lorenzo, F., Armiento, S., Molinaro, A., Marchetti, R., Silipo, A., & De Castro, C. (2022). Liquid-state NMR spectroscopy for complex carbohydrate structural analysis: A hitchhiker's guide. *Carbohydrate Polymers, 277*, Article 118885.

Tschesche, R., Schacht, U., & Legler, G. (1963). Über Daphnorin, ein neues Cumaringlucosid aus *Daphne mezereum*. *Naturwissenschaften, 50*(15), 521–522.

Ulriksen, E. S., Butt, H. S., Ohrvik, A., Blakeney, R. A., Kool, A., Wangensteen, H., … Inngjerdingen, K. T. (2022). The discovery of novel immunomodulatory medicinal plants by combination of historical text reviews and immunological screening assays. *Journal of Ethnopharmacology, 296*, Article 115402.

van Holst, G.-J., & Clarke, A. E. (1985). Quantification of arabinogalactan-protein in plant extracts by single radial gel diffusion. *Analytical Biochemistry, 148*(2), 446–450.

Voragen, A. G. J., Thibault, J.-F., Axelos, M. A. V., Renard, C. M. G. C., & Pilnik, W. (1995). In A. M. Stephen (Ed.), *Food polysaccharides and their applications* (pp. 287–339). London: Marcel Dekker.

Wang, H., Bi, H., Gao, T., Zhao, B., Ni, W., & Liu, J. (2018). A homogalacturonan from *Hippophae rhamnoides* L. Berries enhance immunomodulatory activity through TLR4/MyD88 pathway mediated activation of macrophages. *International Journal of Biological Macromolecules, 107*, 1039–1045.

Wang, T., Wang, X., Zhuo, Y., Si, C., Yang, L., Meng, L., & Zhu, B. (2020). Antiviral activity of a polysaccharide from Radix Isatidis (*Isatis indigotica Fortune*) against hepatitis B virus (HBV) in vitro via activation of JAK/STAT signal pathway. *Journal of Ethnopharmacology, 257*, Article 112782.

Wang, Y.-Q., Mao, J.-B., Zhou, M.-Q., Jin, Y.-W., Lou, C.-H., Dong, Y., Shou, D., Hu, Y., Yang, B., Jin, C.-Y., Shi, H.-C., Zhao, H.-J., & Wen, C.-P. (2019). Polysaccharide from *Phellinus Igniarius* activates TLR4-mediated signaling pathways in macrophages and shows immune adjuvant activity in mice. *International Journal of Biological Macromolecules, 123*, 157–166.

Wefers, D., & Bunzel, M. (2016). NMR spectroscopic profiling of Arabinan and Galactan structural elements. *Journal of Agricultural and Food Chemistry, 64*(50), 9559–9568.

Wold, C. W., Kjeldsen, C., Corthay, A., Rise, F., Christensen, B. E., Duus, J.Ø., & Inngjerdingen, K. T. (2018). Structural characterization of bioactive heteropolysaccharides from the medicinal fungus *Inonotus obliquus* (Chaga). *Carbohydrate Polymers, 185*, 27–40.

Wusigale, Liang, L., & Luo, Y. (2020). Casein and pectin: Structures, interactions, and applications. *Trends in Food Science & Technology, 97*, 391–403.

Xia, Y.-G., Liang, J., Yang, B.-Y., Wang, Q.-H., & Kuang, H.-X. (2015). Structural studies of an arabinan from the stems of *Ephedra sinica* by methylation analysis and 1D and 2D NMR spectroscopy. *Carbohydrate Polymers, 121*, 449–456.

Yamada, H., & Kiyohara, H. (2007). 4.34 - Immunomodulating activity of plant polysaccharide structures. In H. Kamerling (Ed.), *Comprehensive Glycoscience* (pp. 663–694). Oxford: Elsevier.

Yao, H.-Y.-Y., Wang, J.-Q., Yin, J.-Y., Nie, S.-P., & Xie, M.-Y. (2021). A review of NMR analysis in polysaccharide structure and conformation: Progress, challenge and perspective. *Food Research International, 143*, Article 110290.

Yin, M., Zhang, Y., & Li, H. (2019). Advances in research on immunoregulation of macrophages by plant polysaccharides. *Frontiers in Immunology, 10*.

Zhang, H., Li, C., Ding, J., Lai, P. F. H., Xia, Y., & Ai, L. (2020). Structural features and emulsifying stability of a highly branched arabinogalactan from immature peach (*Prunus persica*) exudates. *Food Hydrocolloids, 104*, Article 105721.

Zhang, Y., Zhang, M., Jiang, Y., Li, X., He, Y., Zeng, P., … Zhang, L. (2018). Lentinan as an immunotherapeutic for treating lung cancer: A review of 12 years clinical studies in China. *Journal of Cancer Research and Clinical Oncology, 144*(11), 2177–2186.